Science of the Total Environment 889 (2023) 164095

Contents lists available at ScienceDirect

Science of the Total Environment

journal homepage: www.elsevier.com/locate/scitotenv

Measurement and modeling of water vapor sorption on nano-sized coal particulates and its implication on its transport and deposition in the environment

Sikandar Azam, Shimin Liu *, Sekhar Bhattacharyya, Ang Liu

Department of Energy and Mineral Engineering, G³ Center and Energy Institute, The Pennsylvania State University, University Park, PA 16802, USA

HIGHLIGHTS

- Nano-size coal dust particles can interact with environmental moisture.
- Nano-size lignite coal dust can adsorb 10 times more moisture than bituminous coal dust.
- GAB and Freundlich models are superior to BET models for defining water uptakes.
- Moisture interaction will affect the transport behavior of coal dust in the underground mine environment.

GRAPHICAL ABSTRACT

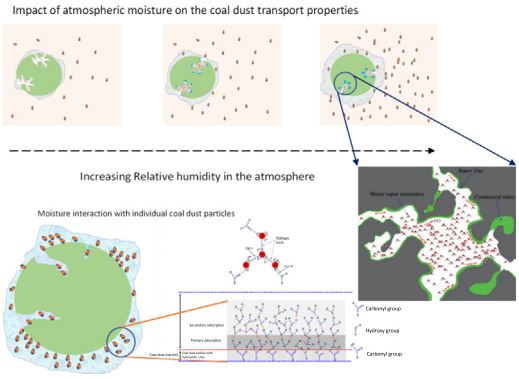

ARTICLE INFO

Editor: Pavlos Kassomenos

Keywords:
Nano-sized coal dust
Moisture
Relative humidity
Mine environment
Underground coal mining

ABSTRACT

One major cyclical environmental parameter within the underground mine space is the fluctuation of relative humidity, which varies daily and seasonally. Therefore, moisture and dust particle interactions are inevitable and indirectly control dust transport and fate. After being released into the environment, the coal dust particles stay there for a long period depending upon several parameters such as particle size, specific gravity, ventilation etc. Due to their smaller size, nano-sized coal dust particles could remain in the mine environment indefinitely while interacting with it. Correspondingly the primary characteristic of nano-sized coal dust particles could get modified. The nano-sized coal dust samples were prepared in the lab and characterized using different techniques. The prepared samples were allowed to interact with moisture using the dynamic vapor sorption technique. It was found that the lignite coal dust particles could adsorb up to 10 times more water vapor than the bituminous coal dusts. Oxygen content is one of the primary factors in deciding the total effective moisture adsorption in the nano-sized coal dust, with moisture adsorption proportional to the oxygen content of the coal. This means that lignite coal dust is more hygroscopic when compared to bituminous coal dust. GAB and Freundlich's models perform well for water uptake modeling. Because of interaction with atmospheric moisture, particularly swelling, adsorption, moisture retention, and particle size changes, such interactions will significantly change the physical characteristics of nano-sized coal dust. This will affect the transport and deposition behavior of coal dust in the mine atmosphere.

* Corresponding author at: Department of Energy and Mineral Engineering, Pennsylvania State University, 224 Hosler Building, University Park, PA 16802, USA.
E-mail address: szl3@psu.edu (S. Liu).

http://dx.doi.org/10.1016/j.scitotenv.2023.164095
Received 20 March 2023; Received in revised form 26 April 2023; Accepted 8 May 2023
Available online 18 May 2023

1. Introduction

Almost all the coal mining processes produce airborne respirable dust, identified as one of the major occupational health hazards impacting workers' health. Coal mine workers work in a condition where they have prolonged interaction with coal dust, and chronic inhalation of coal dust could cause several lung diseases such as coal workers' pneumoconiosis (CWP), progressive massive fibrosis (PMF), chronic bronchitis, lung function loss, and emphysema (RP and PJ, 1999). Recent observations show an increased incidence of CWP or other lung diseases, particularly among young miners in the Appalachian basin. The CWP prevalence in Appalachia is four times higher than the national age-adjusted prevalence rates in the US (5.9 %) (JB et al., 2018). Even with tighter regulation for permissible mine dust limits, the resurgence of such disease among coal miners demands further and detailed efforts to enhance our understanding of the possible facets of coal dust toxicity, taking insights from current interdisciplinary research efforts. The proportion of nano-size coal dust in the mine atmosphere is comparatively higher than micron sized coal dust particles in terms of *number* (Fan and Liu, 2021). Recently, there is a growing concern in the mining community about the contribution of nano-particulates to miner's health because of their specific characteristics. Although nano-scale particulates with complicated physiochemical properties and contributes enormously in quantity, they have been drawing attention only in recent a few years because of the advancement of nano-science discipline. Hence, it is necessary to understand the complete fate of coal dust from its production to deposition.

To summarize the process, coal dust is released during the cutting/extraction of coal. From there, coal dust gets released into the mining environment. Depending on the particle size, these particles could stay in the environment. Then finally, these particles will be inhaled by the mineworkers. Several amounts of research have been done to understand and control the dust generation process in the mining industry (Fan and Liu, 2021; Kossovich et al., 2020; Zhang et al., 2021). Similarly, much work has been done to protect mineworkers from coming in contact with and inhaling coal dust. However, it's almost impossible to find any work which tries to understand the middle and the longest of the whole coal dust generation to inhalation process, which is the stay and transport of coal dust in the environment after generation and before inhalation by workers. It is well known that particulates can stay floating in the environment for months. At the same time, their transport and deposition will be governed by both coal dust and environmental characteristics. One of the key properties that will determine the stay and transport of coal dust particles is their size. It is well-documented that nano-size coal particulates can stay in the environment longer than larger micron-sized particles (Fan and Liu, 2021). The longer they stay, the more they interact with the environment; their primary characteristics will change correspondingly. It is to be noted that most of the lab or toxicity studies consider that the mine workers are inhaling the coal dust generated in the mine while not accounting for the changes they undergo during their stay and transport in the environment before inhalation. This assumption might only be true for larger particles that do not stay in the environment longer. Conversely, nano-size coal dust particles could stay in the atmosphere longer. During their stay, they could interact with the atmosphere. The nano-sized coal dust particles are comparatively more susceptible to the external environment because of their increased pore volume, surface area and, more importantly, an increased proportion of surface atoms (Zhang et al., 2021). It indirectly suggests that the nano-size coal dust particles which are released into the environment are different from what is being inhaled by workers. Hence, we must understand the interaction of coal dust nanoparticles and the environment in which they are released.

As discussed, both environmental and particle characteristics will play an important role in governing the transport and modification of particles in the underground mine environment. Among all the components of mine environment, the moisture content or relative humidity (RH) seems to be one of the critical components. The effect of RH in modifying the overall characteristics of dust particulates released into the underground mine environment has never been understood. However, research conducted in atmospheric sciences in the past decade makes it clear that moisture in the atmosphere can significantly alter the behavior of mineral dust (Chen et al., 2020; Courtney R. Usher et al., 2003; Ibrahim et al., 2018; Joshi et al., 2017; Michel et al., 2003; Seisel et al., 2005; Tang et al., 2016). Thus, the interaction of coal dust with moisture in underground mines should be characterized and quantified. Although moisture is prevalent and dynamic in a mining environment, limited efforts have been devoted to understanding the role of aerodynamic properties of dust (size, shape, specific gravity, surface roughness, etc.) in terms of the dust transport process in the mine air. Indeed such an understanding will go a long way in solving some of the dust-related critical issues in the mining industry. Mine ventilation is well known as one of the costliest affairs of any underground mining company (Grau and Krog, 2008; Oching and Ghomshei, 2019; Pritchard, 2010; Wei et al., 2020). Understanding the transport and interaction behavior of coal dust nanoparticles in the dynamic humid environment could help optimize the ventilation system and reduce the financial burden on the mine operators. In addition, these secondary particles (nano-size coal particles that have stayed and interacted with the environment) might have undergone changes that significantly differ from primary particles. Correspondingly, their health impact might be different. At the least, the interaction of nano-size coal dust particulates with the environmental moisture can significantly change flow dynamics, which will definitely impact the mine ventilation and the inhalation of the particle by the workers (Löndahl et al., 2010; Tu and Knutson, 1984; Varghese and Gangamma, 2009). Moreover, the moisture interaction of coal dust particles in the environment could change how they interact with the dust-suppressing agents (Yu et al., 2022). This will further affect the health impact of these particles.

From these interdisciplinary insights, a fundamental understanding of the moisture sorption behavior of different types of coal dust is extremely important. Different types of coal dust will interact differently with moisture, depending on their primary properties and composition. Hence, as the first step, it is extremely important to understand how much moisture different coal dust produced from different coals can take or, in other words, the sorption and retention behaviors of moisture on different coals.

2. Background and literature review

As discussed above, it's very important to understand the interaction of coal dust nano particulates released into the environment and its associated dynamics of flow behavior in a dynamic humidity environment. A study showed the growth of water film on hydrophilic mineral nanoparticles from water vapor by using infrared nano spectroscopy, amplitude-modulated atomic force microscopy, and molecular simulations (Yalcin et al., 2020). Relative humidity changes could enhance the agglomeration rate of particles because of the increased aqueous liquid bridging force. This can dynamically affect the size distribution of particulate matter in the atmosphere, impacting the mechanism of haze formation, whether in open or underground mines, which could further impact the visibility of workers (He et al., 2019). Some laboratory-scale experiments have demonstrated that the interaction of aerosols with moisture significantly influences the adsorption properties, heterogeneous reactivity and photoreactivity of several mineral dusts (Bedjanian et al., 2013; Crowley et al., 2010). Interested readers may look into comprehensive reviews on the water and dust interactions (Rubasingheghe and Grassian, 2013; Vaida, 2011). Although the interaction behavior of several mineral dusts, such as clay, oxides, nitrogen oxides, carbonates, etc., have been well studied (Hudson et al., 2008; Rubasingheghe and Grassian, 2013). However, similar studies for coal dust are missing or only limited to the mining industry and the researchers. It is well-known that coal dust is much more complex than other single-component mineral dust (Castro-Marcano et al., 2012; Cheng et al., 2017). This means that the interaction of coal dust with moisture is expected to be an even more complex process and thus influences dust transport behaviors. Also, coal dust is not only a problem of the mining industry or workers involved in it; it has also been found to be

prevalent in the neighboring urban population (He et al., 2003; Triantafyllou et al., 2006).

Even the characteristics of coal dust could play a major role in their moisture uptake and interaction behavior. It has been demonstrated that coal dust with higher inherent moisture content is much more easily moistened than dust with lower moisture (Xu et al., 2017). Particle size distribution also impacts the moisture interaction of coal dust. Generally, with a decrease in size, the surface area and pore volume increase and the average pore size decrease leading to an increase in surface roughness. Another study also found that reducing oxygen content will increase the hydrophobicity of coal dust and thus reduce the tendency of moisture to interact with the coal dust (Yang et al., 2010).

Respirable-size coal dust is usually less hygroscopic, emphasizing that hygroscopicity can even be weakened for nano-sized coal dust particles (Wang et al., 2017). As mentioned above, the exposed area of coal dust increases with a decrease in size. Hence, if the coal dust is dominated by carbon-containing groups such as aromatic hydrocarbons containing benzene rings, aliphatic hydrocarbons with methyl, methylene, etc., then the amount of carbon in the surface layer of coal dust increases, decreasing the tendency of coal dust to interact with moisture or making it hydrophobic tendency. However, coal dust with oxygen-containing functional groups (represented by the hydroxyl and carboxyl groups, silicate and carbonate minerals) can be hydrophilic and better interact with environmental moisture (Wang et al., 2017). Another study found that coal with higher volatile content is less hygroscopic due to its ability to release volatile matter to form a gas film around the particle (Li et al., 2013). It was also found that coal dust with simple and few aromatic structures and long side chains have strong hydrophilicity due to the high contents of oxygen-containing functional groups (-COOH and -OH) (Yao et al., 2017). With a decrease in the oxygen-containing functional group, the hydrophilicity decreases. The side chains detach, and only some oxygen-containing functional groups are included in the coal dust, which is dominated by intense aromatic structures of several rings (anthracenes and Phenanthrenes), making them more hydrophobic. Rather surface hydroxyl is the main factor in deciding the hydrophilicity of the coal dust particles (Xu et al., 2017). Overall, the moisture interaction potential of coal dust is extrinsically controlled by the particle size distribution and agglomeration state while intrinsically influenced by the distribution of hydrophilic and hydrophobic functional groups. Moisture present in the environment significantly impacts nano-size coal dust's characteristics, flow behavior, and hygroscopicity.

Several studies have shown that the surface reactivity and free radical properties of mineral dust particles could change because of moisture interactions (Rubasingheghe and Grassian, 2013). The 2018 National Academy of Sciences (NAS) report mentions the changes in the typical dust-size distribution for silica and coal dust due to changes in mining practices, conditions, and technologies (National Academies of Sciences, 2018). These changes in the characteristics of coal dust produced and the realization of the existence of nano-scale coal dust could have several impacts (Fan and Liu, 2021; Liu and Liu, 2020). This could have led to changes in the disease epidemiology, the impact of which might be reflected in the near future. Also, volumes of research on the activity potential of nano-sized material unanimously agree that the activity at the nano-scale is much higher than at the micron scale. Recently, a study characterized micron to nano-sized coal dust using several techniques, including proximate/ultimate analyses, X-ray diffraction (XRD), X-ray photoelectron spectroscopy (XPS), laser diffraction, and low-pressure CO_2 and N_2 adsorption (Zhang et al., 2021). They found that the nano-sized coal dust is much more chemically and physically active than its larger counterpart. Nano-sized coal dust has reduced oxygen-containing functional groups, suggesting a weaker hygroscopic behavior suggesting potentially higher adverse health effects. However, it could happen that due to certain interactions in the atmosphere, the hygroscopicity could increase, and nano-sized dust already has increased pore volume and surface area, which could make them much more reactive.

Nevertheless, based on the discussion above, several hypotheses could be made that might need further investigation. We discussed that the finer-sized coal dust is less hygroscopic and could potentially reach the lung's deepest regions as their particle size distribution will not change much due to less vapor uptake. In contrast, larger-sized coal dust particles could have much more tendency to deposit in the upper region of the respiratory airways. More hydrophilic coal dust particles, even nano-size, could interact intensively with the respiratory tract's relative humidity and grow in size. They could get deposited in the upper region through impaction or sedimentation. In the introduction, we already discussed that the issues related to coal dust in the mining region are getting worse for hot coal mining regions, such as the central Appalachian basin. Modern much-advanced coal extraction practices could have changed the particle size distribution of the production-induced coal dust. Nano-sized coal dust particles are much more active than their larger counterparts (Fan and Liu, 2021; Liu and Liu, 2020; Zhang et al., 2021).

The present study especially focuses on understanding the moisture interaction behavior of nano-sized coal dust. To our knowledge, this is the first attempt at applying several adsorption models to water adsorption to understand the moisture interaction behavior of nano-sized coal dust particles. We quantified the coal dust-specific moisture interaction behavior based on the DVS data. We discussed the implications of such results regarding their effect on the flow behavior of the coal dust and toxicity.

3. Materials and method

3.1. Coal dust preparation

Moisture interaction behavior of coal dust was performed using nano-sized coal dust prepared in the lab from 4 different coal samples. Two bituminous and two lignite coal samples were selected for the study. All four coal samples were obtained from the Pennsylvania State University coal sample bank. The lignite coal samples, labeled as *Lig1* and *Lig2*, were collected from Beulah Seam (Mercer County, North Dakota) and Pust seam (Richland County, Montana). The two Bituminous coal samples, *Bit1* and *Bit2,* were collected from Sewell Seam (Greenbrier County, West Virginia) and Upper Kittanning Seam (Barbour County, West Virginia), respectively. Each coal sample was initially hand-crushed by a pestle and mortar to a particle size of <80 mesh (<177 μm), which was suffixed as a hand-crushed (HC) sample. Each HC sample was further pulverized to get nano-sized coal dust through the cryogenic ball-milling using CryoMill (Retsch Inc.) at the lab. During the Cryomill processing, liquid nitrogen was continuously circulated through the autofill system to keep the temperature at 196 °C during the ball-milling. Using a liquid nitrogen environment prevents the heating of the powder sample, which makes the process faster and maintains the original nanopore structure of the coal dust. A maximum of 20 ml of the HC coal dust powders were put into the sample cell. 5 Hz of vibrational frequency was used for pre-cooling, and four cycles with 2 min of each cycle and 30 Hz of vibrational frequency were used. One minute of intermediate cooling time was kept between each cryo-milling cycle. Such coal dust samples were suffixed as Cryomill 4 cycle (Cr4) samples.

3.2. Characterization of chemical properties of all coal samples

Each coal sample's petrophysical and petrochemical properties were obtained from the coal sample bank datasheets. Some important properties used throughout the paper were presented and discussed here.

3.2.1. Proximate, ultimate, and elemental analysis

Table S1 shows the proximate, ultimate and elemental analysis data of the coal samples as obtained from the coal sample bank. Two lignite samples, Lig1 and Lig2, have low carbon content, 22.89 % and 30.5 %, respectively, for the as-received samples as determined from proximate analysis. In comparison, two Bituminous coal samples have much higher carbon content than the two lignites, 69.77 % and 56.06 %, respectively. Another important feature is that the proximate analysis shows heavy moisture content in these two lignites at 33.38 % and 34.91 %, compared to the two bituminous coals with 1.45 % and 1.46 %, respectively. Similarly, the ultimate

analysis of the samples shows a much higher oxygen content of 12.40 % and 10.50 % for the two lignites compared to the two bituminous coal, which only has 4.44 % and 5.17 %, respectively. In terms of elemental carbon and oxygen, we again observe the same trend that the lignite coals have lower elemental carbon and higher elemental oxygen content. Several other elements, such as Nitrogen and Sulfur, are present in the coal samples. The amount of nitrogen is slightly higher in the Bit1_Cr4 and Bit2_Cr4 samples at 1.44 and 1.3 compared to the Lig1_Cr4 and Lig2_Cr4, which has 0.9 and 0.94 %, respectively. The difference in the carbon and oxygen content of the bituminous and lignite coal samples is expected because of the coal rank difference. Bituminous coal has undergone more maturity, and because of the longer coalification process than lignite, it has become more dense, dry and rich in carbon (Liu et al., 2021).

3.2.2. Atomic ratios and reflectance

Table S2 shows the important atomic ratios and vitrinite reflectance of the coal samples. As mentioned by the previous studies, the O/C ratios could represent the surface hydrophilicity of the coal matrix of three coal samples (Buchner et al., 2016; Kovtun et al., 2019). In general, lignites have higher atomic H/C and O/C ratios than the two bituminous coal dust samples, except Bit2 coal, which has a higher H/C ratio (H/C = 0.77) than Lig1 (H/C = 0.732). More maturity of the bituminous coal is depicted by their higher reflectance values of 1.35 and 1.07 compared to the two lignites, 0.35 and 0.23, as mentioned in Table S2. As per the Van Krevelen diagram, the rank of the studied coal samples is Lig1 is lignite-A, Lig2 is lignite-A, whereas Bit1 is medium volatile bituminous and Bit2 is high volatile-A bituminous.

Chemical characterization of coal samples suggests that the molecular structures of the two lignites are much more heteroatomic and aliphatic or have more side chains. In contrast, the two bituminous coal samples are much more aromatic and less heteroatomic. We will discuss the implications of these observations in subsequent sections.

3.3. Analysis techniques

3.3.1. Particle size analysis of the crushed coal dust samples

As described earlier, each of the four coal samples was initially hand-crushed and then cryo-milled for four cycles. Two measurement techniques were used to confirm the dominating presence of the nano-sized coal dust in the samples. The particle size distribution for these samples was measured by both Mastersizer 3000 and Zetasizer Nano ZS located at the Materials Characterization Lab of Penn State. Mastersizer 3000 is based on the Dynamic Light scattering technique, whereas Zetasizer Nano ZS is based on the laser diffraction technique.

Before each measurement, each coal dust sample (dispersant) and isopropanol (solvent) were mixed inside a small beaker and put in an ultra-sonic oscillator for about 5 min for preliminary dispersion purposes. The solvent with dispersant was then put into a flow cell containing pure solvent only for the measurement. Mastersizer 3000 software (v3.81) was used for data collection and particle size analysis. Non-spherical particle type was chosen for data analysis to obtain accurate size distributions for all the hand-crushed and milled samples. The same procedure was followed to measure particle size distribution using Zetasizer Nano ZS; however, less sample quantity was required. The samples were put in a 12 mm OD (outer diameter) square polystyrene cuvette for aqueous solvents for measurement. Zetasizer software (v8.01) was chosen for data collection and particle size analysis.

3.3.2. Dynamic vapor sorption analysis and ad-/desorption isotherm

The moisture interaction behavior of the coal dust samples was studied with the help of the DVS method. Water sorption experiments were performed using the DVS intrinsic Plus instrument Surface Measurement Systems Ltd. The Dynamic Vapor Sorption (DVS) Intrinsic accurately measures the mass changes of the sample under different relative humidity, the water vapor ad/desorption isotherms and kinetics at each relative humidity step. The DVS sorption and desorption isotherm was obtained for each coal dust sample at 30 °C. A gas flow stream with a fixed flow rate of 200 standard cubic centimeters per minute (sccm) was continuously supplied into the sample chamber for each experiment. The relative humidity, equivalent to the partial pressure ratio of water vapor, was adjusted by two mass flow controllers by mixing a dry N_2 stream with a wetting N_2 stream containing 100 % humidity. Dynamic changes in mass under different relative humidities were measured by microbalance with a sensitivity of 0.1 μg ± 1 %. Dry purge gas constantly flowed through the balance chamber at a rate of 70 ± 10 sccm and a temperature of 40 °C to avoid potential vapor condensation in the balance chamber and ensure optimal microbalance performance. Once the conditions of the DVS instrument were set as described above, a coal dust sample weighing between ~20–50 mg was loaded onto a small pan suspended on the microbalance. The experiments started at ~0 % RH, at which it is assumed that the residual water desorbs to reach an equilibrium state. The mass of the sample at the end of this stage is considered the mass of the dry sample. Further changes in the mass during the adsorption and desorption cycle are evaluated from this reference mass. Further Experimental details are provided by Sang et al., 2019; Seemann et al., 2017.

4. Results and discussions

4.1. Particle size analysis of coal dust samples

As described, we carefully prepared the nano-sized coal dust particles to understand the moisture interaction. Isopropanol was used as the solvent per a previous study's recommendation (Zhang et al., 2021). Particle size distributions were obtained using Malvern Panalytical Mastersizer, and Zetasizer, shown in Fig. 1. The particle size measurement range of the Mastersizer is 0.01–3500 μm. The operating principle of the Mastersizer allows it to provide better particle size distribution information for the larger particles in the sample as they scatter more light than the smaller particles. The number distribution in Fig. 1 shows that most large particles that dominate the laser diffraction are smaller than 1000 nm (1 μm). This means the samples are dominated by <1000 nm (1 μm) sized particles. Although some >1000 nm (1 μm) particles are measured by the master sizer, their numbers are insignificant. It is clearly understood that these few large particles will occupy most of the volume, and hence not surprisingly, the volume distribution for all four coal dust samples is mostly >1000 nm (1 μm). Another key feature is a single and sharp peak for number distribution at <1 μm for all the coal dust samples, whereas the volume distribution shows a broad distribution range. The details of the observations are also presented in Table S1 for the Mastersizer.

The inner graphs in Fig. 1 for all four coal dust samples show the particle size distribution measured using Malvern Zetasizer in the range marked by the arrows. The typical measurement range of a zeta-sizer is 0.3 nm to 10 μm, and it is considered a crucial instrument for measuring the particle size of nano-scale particles. The particle size measurement of the Zetasizer is based on the principle of dynamic light scattering (DLS). A small amount of the sample was dispersed in the isopropanol solvent and left undisturbed for 2 min to stabilize the dispersion. Thermally-induced collisions between solvent molecules and the dust particles cause the suspended coal dust particles to undergo Brownian motion. As per the principle of DLS, when these randomly moving particles are illuminated with a laser, the intensity of the scattered light fluctuates over time at a rate dependent upon the particle size. As can be understood, the smaller particles are displaced by the solvent molecules more than the large particles because of Brownian motion and hence move more rapidly.

Analysis of these intensity fluctuations yields the Brownian motion's velocity and particle size using the Stokes-Einstein relationship. Note that the diameter measured in DLS is termed the hydrodynamic diameter and refers to how a particle diffuses within a fluid. Therefore, it can be understood from the working principle of the Zetasizer that it is more sensitive toward smaller particles than the larger particles in the coal dust samples. Number distribution in the inner graphs of Fig. 1, we again observe that maximum particles are <1000 nm for all four coal dust samples. Also, the number distribution

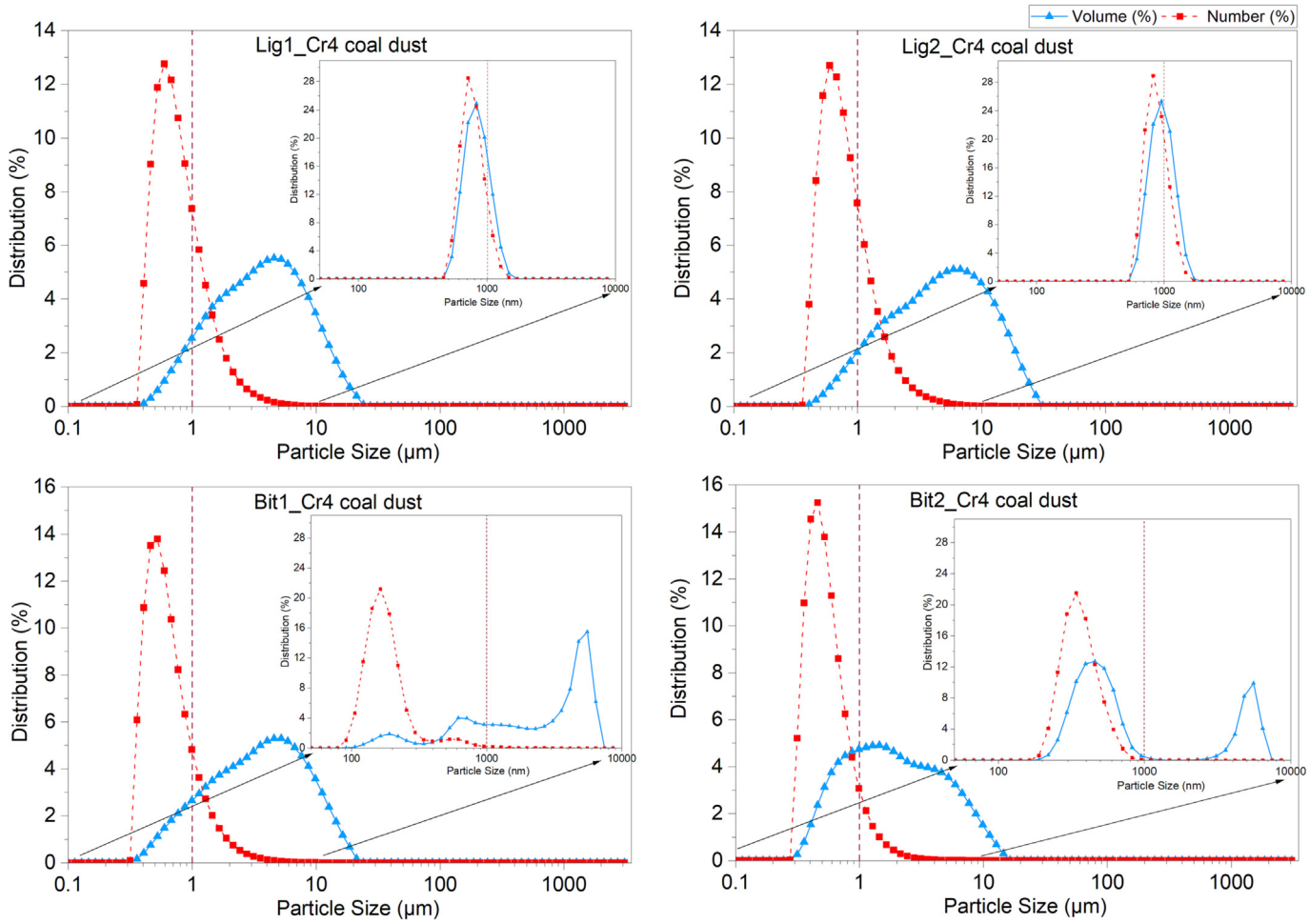

Fig. 1. Particle size distribution for different coal dust samples measured using Mastersizer. The inside graphs represent the particle size distribution measured using the Zetasizer for the marked range.

has sharp peaks. The volume distribution for the Lig1_Cr4 and Lig2_Cr4 samples also has a single peak at a value <1000 nm, whereas the Bit1_Cr4 and Bit2_Cr4 samples have broad and multiple peaks. Here again, not surprisingly, a small number of particles have occupied most of the volume, and hence we see such a volume distribution measured by the Mastersizer.

The use of two powerful particle measurement techniques was chosen to describe the particle size of the coal dust samples in detail, both at nano-scale and micron-scale levels. The measurements showed that the coal dust preparation technique was properly designed and yielded the desired result for excessive nano-sized particle preparation.

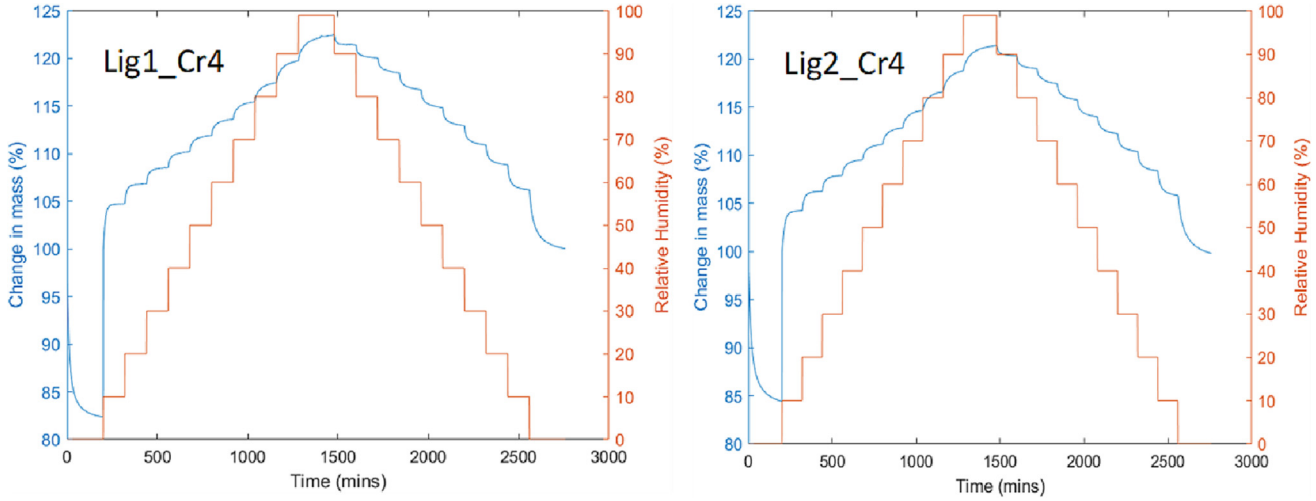

Fig. 2. Typical water vapor sorption plot using DVS—raw data recovered from the dynamic vapor sorption analyzer for the Lig1_Cr4 and Lig2_Cr4 coal dust sample at 30 °C.

4.2. Moisture ad-/desorption and diffusion measurements

4.2.1. Dynamic vapor sorption measurements on nano-sized coal dust

All ad-/desorption data for the nano-sized coal dust samples were collected using the DVS method. Fig. 2 shows typical sorption plots obtained using the dynamic water vapor system. Initially, the experiments started at 0 % RH, which was kept for around 3 h to remove any residual water from the coal dust. Based on the ad-/desorption cycle, hysteresis plots were created for all the samples shown in Fig. 2.

It is apparent from Fig. 2 that all the coal dust took up significant quantities of water vapor, and the measured water content increases with increasing R_H. The two lignites have higher water uptakes, taking >0.20 g (moisture)/g (coal dust) of humidity at 99 % RH. In comparison, Bit1_Cr4 and Bit2_Cr4 only take approximately 0.02 g (moisture)/g (coal dust) of moisture at 99 % RH. However, there is a slight difference in the adsorption pattern and maximum adsorption of Lig1_Cr4 and Lig2_Cr4 and similarly between Bit1_Cr4 and Bit2_Cr4. Also, we see that even at 99 % RH, no plateau is reached. Looking at Fig. 3 and Table S4, it can be roughly observed that the water adsorption for Lig1_Cr4 and Lig2_Cr4 is approximately ten times higher than the Bit1_Cr4 and Bit2_Cr4. (Jiang et al., 2020; Xu et al., 2017). Fig. 3 also demonstrates that the water uptake increases initially at low RH in a non-linear convex fashion, followed by an upward concave increase at high R.H. Overall, the total water uptake differences are significant for the two bituminous and two lignite coal dusts.

The results show that the Lig1_Cr4 and Lig2_Cr4 samples could take >0.1 g (moisture)/g (coal dust) at 50 % RH Comparatively, Bit1_Cr4 and Bit2_Cr4 samples take even <0.015 g (moisture)/g (coal dust) of moisture at the same RH Also measured values were the adsorbed water contents on coal dust upon decreasing the RH to probe for any hysteresis in the adsorption and desorption branches of the water content curves. According to the IUPAC classification, all the nano-sized coal dust samples exhibit an H4-type hysteresis loop suggesting the process of capillary condensation in mesopore structure (Sing, 1985). The H4-type loop is often associated with narrow slit-like pores (Sing, 1985). Earlier studies have shown that the monolayer adsorption on primary adsorption sites and further secondary adsorption on them governs the shape of the isotherm (Du and Wang, 2021; Liu et al., 2021). This is because the water molecule is polar, and they are inclined to form hydrogen bonds with other molecules or functional groups (Du and Wang, 2021). This hydrogen bonding tendency of the hydrogen molecule leads to the development of secondary adsorption sites. In the coming sections, we will discuss various models and their fit integrity as described by Hatch and coworkers, suitably describing nano-size coal dust ad-/desorption behavior (Hatch et al., 2012).

4.2.2. BET sorption analysis

Brunauer–Emmett–Teller (BET) theory which was developed by Brunauer et al., extends the Langmuir mechanism from a localized monolayer model to multilayer adsorption and obtains an isotherm equation (the BET equation), which has the Type II character (Brunauer et al., 1938; Rouquerol et al., 2013). It is the most frequently applied method to understand the sorption properties of many materials. Monolayer capacity (Q_m) and the specific surface area (SSA_{BET}) can be calculated using the BET equation given as follows:

$$\frac{Q}{Q_m} = \frac{C(p/p^o)}{(1-p/p^o)(1-p/p^o+C(p/p^o))} \tag{1}$$

Eq. (1) can be written in the usual linear form:

$$\frac{p}{Q(p^o-p)} = \frac{1}{Q_m C} + \left(\frac{C-1}{Q_m C}\right)\frac{p}{p^o} \tag{2}$$

where Q is the adsorbed amount ($mmol\ g^{-1}$), Q_m denotes the monolayer capacity ($mmol\ g^{-1}$), C is the BET empirical constant which indicates the order of the magnitude of the attractive adsorbent-adsorbate interactions. It is related to the enthalpy of adsorption for the first molecular layer of

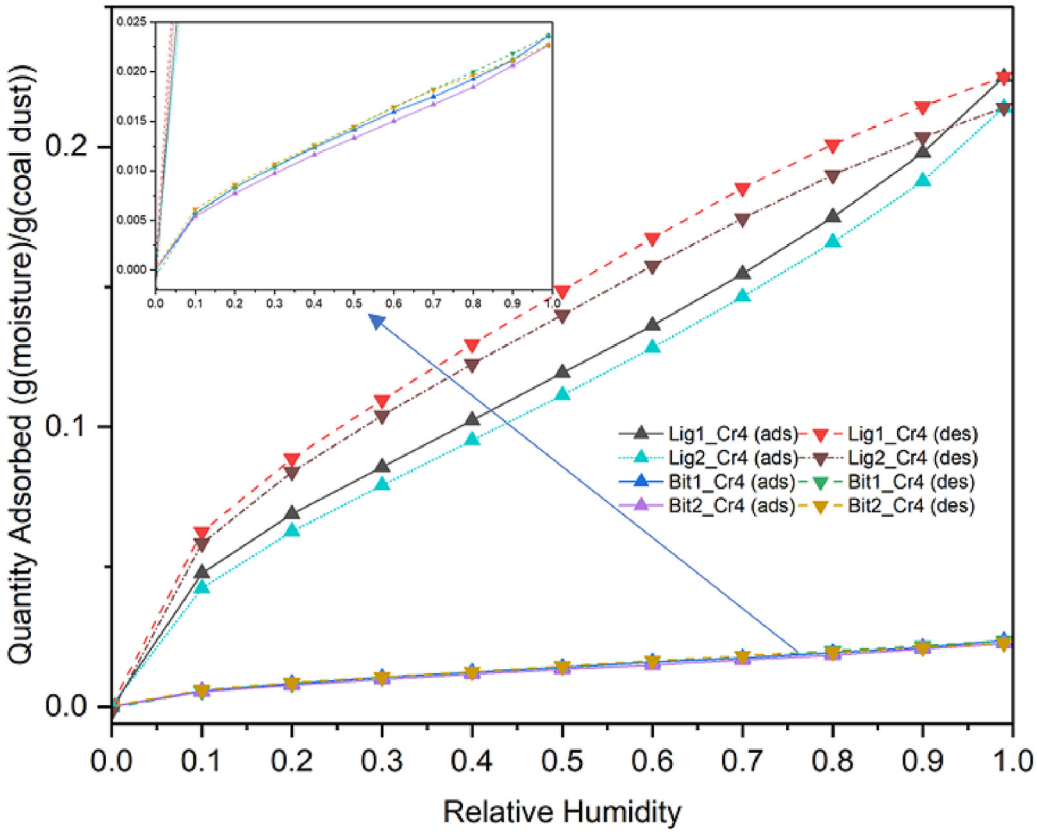

Fig. 3. Dynamic vapor sorption isotherms for different coal dust samples.

water and the enthalpy of adsorption for subsequent layers described as (Hatch et al., 2012):

$$C = \exp\left[\frac{\Delta H_2^0 - \Delta H_1^0}{RT}\right] \quad (3)$$

where R (J/mol.K) is the universal gas constant, T (K) is the temperature, ΔH_1^0 (J) is the enthalpy of adsorption of the first layer, ΔH_2^0 (J) is the standard enthalpy of adsorption on subsequent layers and is taken as the standard enthalpy of condensation. As per Eq. (2), a linear plot between $\frac{p}{Q(p^o - p)}$ and $\frac{p}{p^o}$ should provide the BET plot of experimental isotherm data and corresponding Q_m and C. For DVS experiments $\frac{p}{p^o}$ denotes relative humidity R_h. Specific surface area is given by

$$SSA_{BET} = Q_m A_n \sigma \quad (4)$$

where A_n is the Avogadro's constant taken as 6.022×10^{23}, and σ is the so-called cross-sectional area of water taken as 10.5 A^2(the average area occupied by each water molecule in a completed monolayer). An improvement in the accuracy and reproducibility of the BET calculations can be obtained by constraining the fitting interval because the BET equation must be applied to a straight part of the BET plot. For this, the present study used a self-consistency criterion known as the Rocquerol plot method (Rouquerol et al., 2007; Rouquerol et al., 2013). With the help of the Rocquerol plot, the best region where the BET plot is linear is located, and that region is used for the subsequent calculation. Also, the BET model was applied to both sorption and desorption data collected from the DVS analysis for comparison. The best-fit equation was used to get the slope and intercept for the linear fit on adsorption and desorption data. Monolayer coverage $Q_{m(BET)}$ (g (moisture)/g (coal dust) of moisture) and parameter C_{BET} was derived from the slopes and the y-intercepts of the fit lines. Finally, the RH at which monolayer adsorption occurs was determined from the model fit and calculated $Q_{m(BET)}$ values. Table S5 reports the BET-derived parameters, including specific surface area (SSA_{BET}, cm^2/g), monolayer water content ($Q_{m(BET)}$, g (moisture)/g (coal dust)), % RH at monolayer coverage, and correlation coefficient (%R^2) for the linear BET region for all the coal dust samples. Fig. 4 demonstrates the corresponding $Q_{m(BET)}$ and C_{BET} values. It was found that the BET predicted monolayer capacity of the Lig1_Cr4 and Lig2_Cr4 is 0.0697 and 0.0658 (g (moisture)/g (coal dust) of moisture), respectively. Whereas for Bit1_Cr4 and Bit2_Cr4, monolayer capacity is only 0.0085 and 0.0079 (g (moisture)/g (coal dust)) of moisture. Also, there is a large difference in the estimated $Q_{m(BET)}$ from adsorption and desorption isotherm, which is more pronounced for the lignite coal dust (see yellow arrows in Fig. 4).

That is another reason which makes it extremely important to account for the moisture interaction of ultrafine particles to understand better their flow and deposition properties in the mine environment. Since the lignite coal dust particles adsorbed more moisture, their characteristics may get altered more compared to the bituminous coal dust particles. This will lead to a decrease in porosity at higher RH (99 %). Hence, some moisture will be permanently inaccessible during desorption due to the closing of pores. Because of this the $Q_{m(BET)}$ calculated from the desorption isotherm is higher than the adsorption isotherm (Fig. 4). The ratio of maximum adsorption at 99 % RH to the monolayer capacity is 3.23, 3.25,2.76 and 2.85 for Lig1_Cr4, Lig2_Cr4, Bit1_Cr4 and Bit2_Cr4, respectively. Interestingly, although the maximum adsorption capacities of the two-lignite dust are approximately ten times higher than the two-bituminous coal dust, the ratios of the max adsorption to the monolayer capacity are not far from each other. Also, there is a slight difference in the monolayer values calculated from the adsorption and the desorption data for each coal dust. The monolayer values are generally higher for those calculated using desorption than the adsorption data for all the coal dust, as shown in Fig. 4. Similarly, C_{BET} are also higher for the desorption data, with only one exception for Bit1_Cr4 coal dust, for which the desorption C_{BET} is slightly lower than the adsorption C_{BET}. It was also observed that the differences in the desorption and adsorption C_{BET} values are proportional to the ratio of maximum adsorption ($Q_{max\ (BET)}$) and monolayer adsorption ($Q_{m(BET)}$) capacity for nano-sized lignite and bituminous coal dust. $Q_{max\ (BET)}/Q_{m(BET)}$ is in the order of Lig2_Cr4 > Lig1_Cr4 and Bit2_Cr4 > Bit1_Cr4, corresponding to the differences in the desorption and adsorption C_{BET} as can be examined in Fig. 4 and Table S5. It was found that the C_{BET} values are >1 for all the four-coal dust for both the adsorption and desorption cycle, which means that the nano-sized coal dust has type II multilayer water adsorption behavior (Hatch et al., 2012). Another interesting observation is that the estimated specific surface area (SSA_{BET}) calculated using the adsorption and desorption cycles is notably

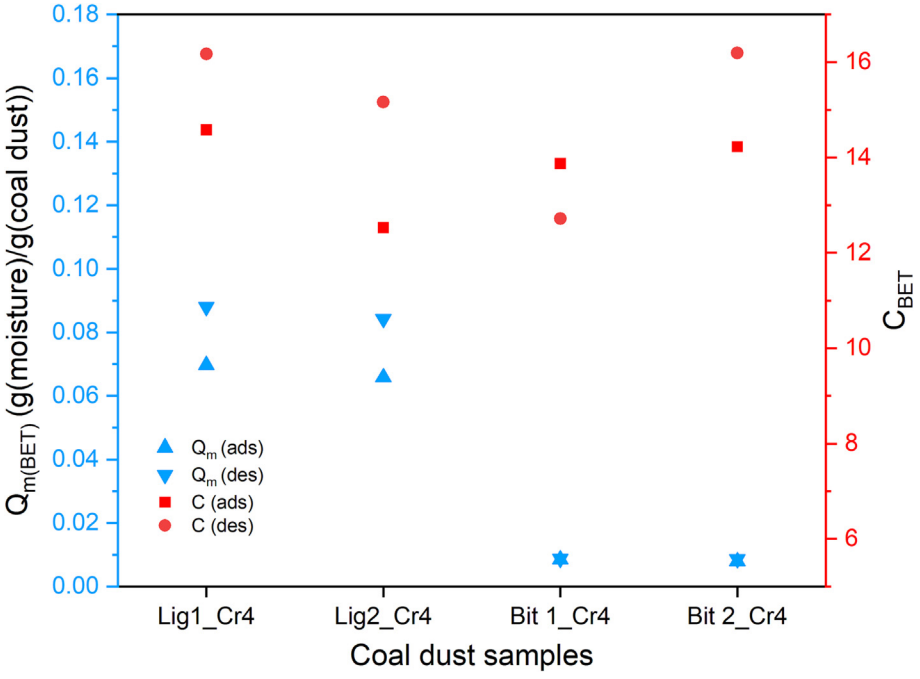

Fig. 4. Monolayer capacity and constant C obtained from BET fits.

different, as reported in Table S5. Moreover, estimated SSA_{BET} calculated from the desorption cycle is greater for all four nano-sized coal dust samples. Also, estimated SSA_{BET} for the two-lignite coal dust (Lig1_Cr4 and Lig2_Cr4) is at least 10 times the estimated SSA_{BET} for the two Bituminous coal dust (Bit1_Cr4 and Bit2_Cr4). As mentioned above, the water molecules are polar, so their adsorption on the coal surface is qualitative and can provide us insightful information about the surface feature of the coal dust. The discussion section will describe the correlation between the coal dust characteristics and the adsorption tendency. However, the similar water sorption tendency of the two lignites and the two bituminous coal dusts signifies that the external properties of the coal dust drive their water interaction behavior, including composition and surface area (Hatch et al., 2012).

The $\%R^2$ for the BET fit is >99.9 % for both the adsorption and desorption fits, as shown in Table S5. Fig. 5 shows the agreement between DVS ad-/desorption isotherm and the corresponding values calculated using BET theory. It was found that the ad-/desorption values modeled by the BET model are in line with the DVS reported values till 40 % RH for all four coal dust. BET-modeled values started deviating from the reported value beyond 40 % RH and became irrelevant at higher R.H. Fig. 5 also shows the % RH at monolayer coverage for the coal dust. For Lig1_Cr4 and Lig2_Cr4, monolayer coverage estimated from the adsorption data is 20.75 % and 22.03 % RH, respectively, slightly higher than that found using desorption data which are 19.92 % and 20.43 %, respectively. However, no significant difference was observed for Bit1_Cr4 and Bit2_Cr4 coal dust as both adsorption, and desorption % RH at monolayer capacity are close to 21 % and 20 % RH, respectively. Interestingly, the differences in the RH at monolayer coverage from adsorption and desorption DVS data are found to be correlated with the degree of hysteresis. Lig1_Cr4 and Lig2_Cr4 samples showed a higher degree of hysteresis; hence, they have larger differences in the BET calculated monolayer coverage RH values compared to Bit1_Cr4 and Bit2_Cr4. The differences in the adsorption and desorption can also be attributed to the swelling and shrinkage property of coal. At higher relative humidity, if the coal dust has a tendency to adsorb more moisture as with lignite coal dust, then many of the pores will be blocked, as can be understood from Fig. 9.

Once the desorption process starts, it won't be possible to completely force this trapped moisture into the inaccessible or closed pores. Because of that, a significant amount of moisture will remain attached to the coal dust, which is one of the reasons that cause the hysteresis between adsorption and desorption curves. The differences in the adsorption and desorption curves are also related to the total moisture sorption capacity of the coal dust. In the present study, we see that the lignite coal dust tends to adsorb more moisture, and the corresponding difference between the ad-/desorption curves is also higher (Fig. 3). Such swelling of coal dust could have possible implications for the flow and deposition behavior of coal dust as will be discussed later. Overall, Fig. 5 shows that the BET model fits the reported data well at lower RH values, after which an upward

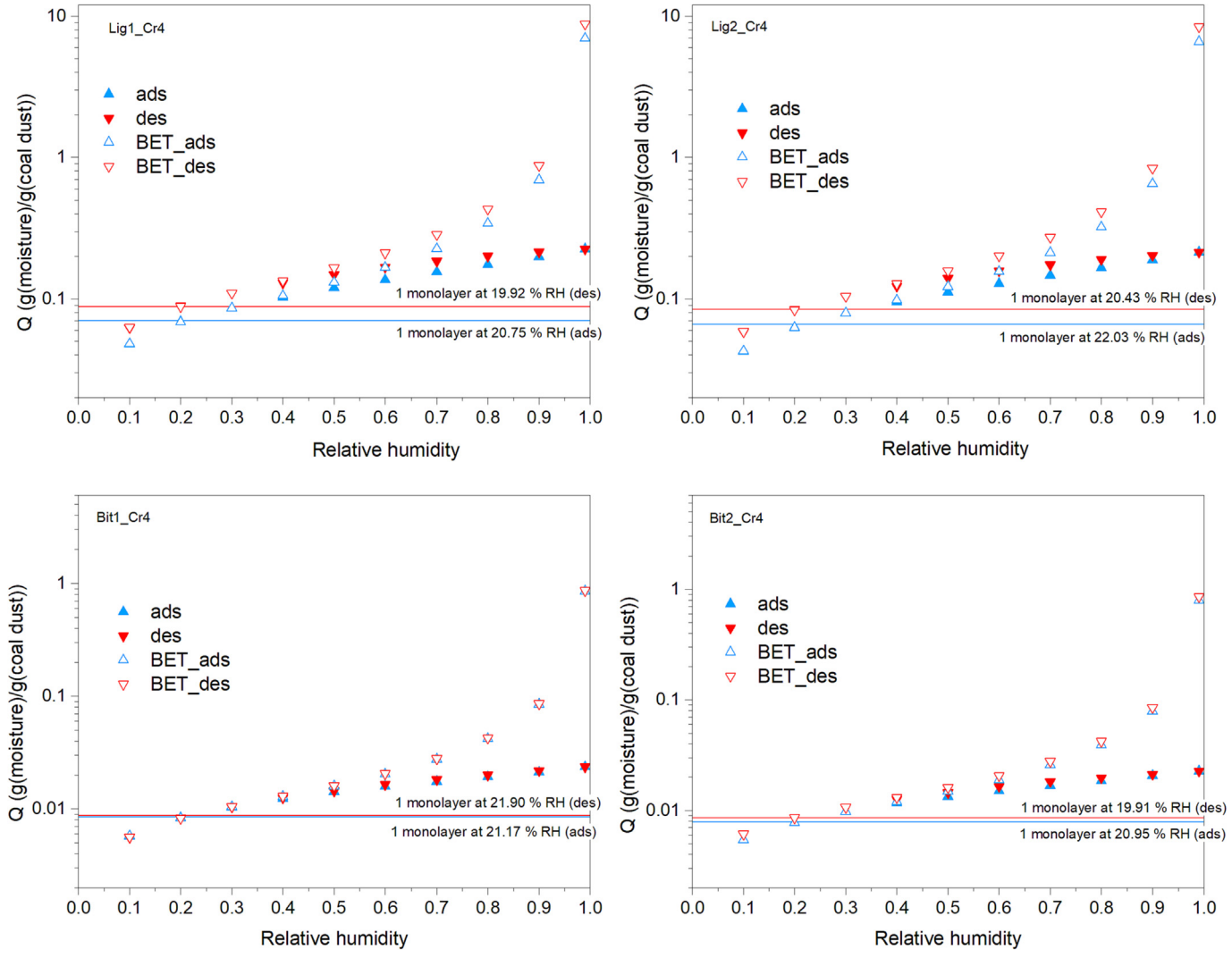

Fig. 5. Ad-/desorption isotherm obtained from the DVS and BET fit. (ads, des represents adsorption and desorption isotherms collected from the DVS data; BET_ads, BET_des represents adsorption and desorption calculated using BET method).

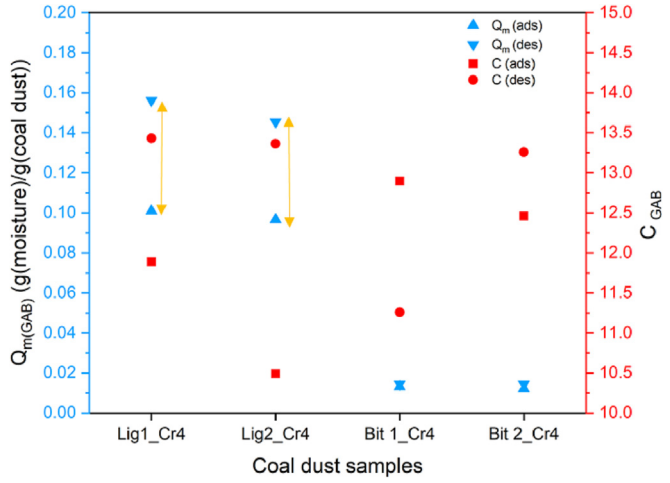

Fig. 6. Monolayer capacity and constant C obtained from GAB fits.

curvature is observed. This deviation indicates that, at higher RH, less vapor is adsorbed than that shown by the BET equation using the values of the constants corresponding to the low activity range.

4.2.3. GAB sorption analysis

The GAB model (Anderson, 1946; DEBOER, 1953; Guggenheim, 1966) is a classical extension of the BET model, which applies to a broad range of relative humidity. BET surface area is deficient as the obtained surface area is an effective probe-specific area rather than a true physical area (Thommes and Cychosz, 2014). Also, BET theory assumes that the heat of adsorption for only the first layer is higher than liquefaction energy for further layers; it is equal to the heat of liquefaction. In contrast, the GAB model assumes that the heat of adsorption of the second and/or higher multilayers is less than the heat of liquefaction, implying that sorbate molecules beyond monolayer adsorption continue to interact with the sorbent surface. Several authors have discussed the applicability of BET theory and its limitations (Rouquerol et al., 2007; Rouquerol et al., 2013; Thommes and Cychosz, 2014). GAB model takes an additional parameter K as expressed in the equation

$$\frac{Q}{Q_m} = \frac{KC(p/p^o)}{(1 - K(p/p^o))(1 - K(p/p^o) + CK(p/p^o))} \quad (5)$$

Q_m and C are similar to those in the BET equation. Additional parameter K compensates for the assumption that the sorption state of the water molecules in the layers beyond the first is the same but different from that of the pure liquid state (Arthur et al., 2018). Specific Surface area can be calculated using Eq. (4) in which Q_m is the monolayer capacity calculated using the GAB equation. The GAB model was also applied to both sorption and desorption data collected from the DVS analysis for comparison. The linearized form of Eq. (5) was used to find the best-fit equation. We can get the slope and intercept for the linear fit on adsorption and desorption data. Monolayer coverage $Q_{m(GAB)}$ (g (moisture)/g (coal dust) of moisture), parameter C_{GAB} and constant K was derived from the best-fit equation. Finally, the RH at which monolayer adsorption occurs was determined from the model fit and calculated $Q_{m(GAB)}$ values. Table S6 and Fig. 6 report the GAB model-derived parameters, including monolayer water content ($Q_{m(GAB)}$, g (moisture)/g(coaldust) of moisture) constant C_{GAB} and correlation coefficient (%R^2) for all the coal dust samples.

Table 1 shows the specific surface area (SSA_{GAB}, cm^2/g), % RH at monolayer coverage calculated using GAB model values.

Like BET results, it was found that the monolayer capacities for the Lig1_Cr4 and Lig2_Cr4 (0.1010 and 0.0966 g (moisture)/g (coal dust) of moisture, respectively) coal dust are much higher than the two bituminous coal dust (0.0132 and 0.0122, respectively). Among the lignite coal dust, $Q_{m(GAB)}$ for Lig1_Cr4 is greater than Lig2_Cr4, similar to the BET calculated values. Similarly, $Q_{m(GAB)}$ for Bit1_Cr4 is slightly larger than the Bit2_Cr4, which is similar to the BET isotherm values, as shown in Table S5. However, $Q_{m(GAB)}$ given by GAB isotherm are always larger than the monolayer value $Q_{m(BET)}$ corresponding to the BET isotherm. Some other studies report similar results for different materials (Ikhu-Omoregbe, 2007; Ocieczek and Zieba, 2020). Also, the $Q_{m(GAB)}$ calculated from the desorption DVS data is higher for the two Lignite coal dust (0.1561 and 0.1455, respectively). A similar observation was made for BET also, and a possible reason has been explained in the earlier section (Section 4.2.2.). Interestingly, that is not the case with the two bituminous coal dust as the $Q_{m(GAB)}$ calculated from the desorption isotherm is lower than those calculated from the adsorption values. However, the difference is not as pronounced as for the lignite coal dust. This observation is different from the BET as GAB analysis reported that the adsorption monolayer values were notably higher for all the coal dust, as shown in Fig. 6.

The constant C_{GAB} from the GAB model have the same physical meaning as that of C_{BET} from the BET model. From Eq. (3), we can easily see that the large C values indicate that water is more strongly bound in the monolayer, and the difference in enthalpy between the monolayer molecules and the subsequent layers is larger. For the nano-sized coal dust samples investigated, C_{GAB} are smaller than the C_{BET} for the adsorption. Similarly, $C_{GAB}$are smaller than C_{BET} except for Bit2_Cr4 coal dust, for which $C_{GAB} > C_{BET}$. This might be because of the slightly uneven desorption curve obtained from DVS around 60–70 % RH, and the corresponding GAB modeled values are also slightly deviating from the observed values. Similarly, C_{GAB} are also higher for the desorption data, with only one exception for Bit1_Cr4 coal dust, for which the desorption C_{GAB} is slightly lower than the adsorption C_{GAB}. A similar trend was observed in the BET analysis, too. Similar to the BET analysis, it was found that the C_{GAB} values are >1 for all four coal dusts for both adsorption and desorption cycles, meaning that the nano-sized coal dust has type II multilayer water adsorption behavior (Hatch et al., 2012).

It was found that there is a notable difference in the specific surface area (SSA_{GAB}) and the RH monolayer content was calculated using adsorption and desorption, as reported in Table 1.

Moreover, SSA_{GAB} calculated from the desorption cycle is remarkably greater for all four nano-sized coal dust samples, and the difference is larger than what was observed for BET analysis. Also, similar to BET observations SSA_{GAB} for the two-lignite coal dust (Lig1_Cr4 and Lig2_Cr4) is at least ten times the SSA_{GAB} for the two Bituminous coal dust (Bit1_Cr4 and Bit2_Cr4). Another important term in the GAB model is the K value. The

Table 1
Specific Surface Area (SSA) and critical relative humidity($RH_{c(GAB)}$) for monolayer sorption calculated from GAB model.

Coal dust samples	GAB model			
	Adsorption		Desorption	
	SSA_{GAB} (cm^2/g)	$RH_{c(GAB)}$ (%)	SSA_{GAB} (cm^2/g)	$RH_{c(GAB)}$ (%)
Lig1_Cr4	3.5466×10^6	38.36	5.4773×10^6	54.10
Lig2_Cr4	3.3891×10^6	40.15	5.1073×10^6	52.98
Bit1_Cr4	4.6335×10^5	44.69	5.0801×10^5	50.10
Bit2_Cr4	4.2803×10^5	43.25	5.0939×10^5	49.86

value of K accounts for the fact that the sorption energy beyond the monolayer is smaller than that of liquefaction. It has been reported that the observed differences in the calculated value of C_{GAB} and C_{BET} can be because of the K values. The value of K reduces as more molecules are grouped in a multilayer and are closer to unity as the difference between the molecules in the monolayer and the bulk liquid becomes negligible (Arthur et al., 2018). When $K = 1$, the GAB equation becomes similar to the BET equation, as shown in Eqs. (1) and (5). It was found that for all the nano-sized coal dust samples examined, the K was <1. This suggests that the water molecules within the monolayer were more strongly bound than those in the multilayer. This goes against the hypothesis of the BET theory, as described at the start of this section. In general, K increases with the increasing strength of water molecules (sorbate) and the surface of the coal dust (sorbent). Table S6 shows that for the coal dust samples, the adsorption K values are larger than the desorption K values. Also, the adsorption K values for two lignite coal dust samples (Lig1_Cr4 and Lig2_r4) are larger than the two bituminous coal dust samples (Bit1_Cr4 and Bit2_Cr4). The larger K values for lignite coal dust samples could mean stronger interactions between sorption sites and water molecules, or the difference between the molecules in the monolayer and the bulk liquid is less for the two lignite coal dust samples when compared to the two bituminous coal dust samples.

The differences in adsorption and desorption values from GAB and BET could be observed for several reasons. The adsorption isotherm is extremely sensitive to the initial water content of the coal dust hydrophilicity of the surface and is also more challenged by stronger intermolecular forces (Johansen and Dunning, 1957; Lu et al., 2015). However, desorption depends not much on these factors as it has already undergone an adsorption cycle.

The $\%R^2$ for the GAB fit is >99 % for both the adsorption and desorption fits, as shown in Table S6. Fig. 7 shows the agreement between DVS ad-/desorption isotherm and the corresponding values calculated using GAB theory. It was found that the ad-/desorption values modeled by the GAB model align with the DVS reported values almost for the complete range of relative humidity (0.1–0.99) for all four-coal dust.

This is significantly different from BET observations, where the modeled values started to deviate from the observed values after 40 % RH This shows that in terms of isotherm modeling for a higher range of RH, GAB is superior to BET. Fig. 7 also shows the % RH at monolayer coverage for different coal dust. For Lig1_Cr4 and Lig2_Cr4, % RH at the monolayer coverage calculated from the adsorption (38.36 % and 40.15 % RH, respectively) is notably lower than that found using desorption data (54.10 % and 52.98 %, respectively). Similarly, for Bit1_Cr4 and Bit2_Cr4, the % RH at adsorption monolayer coverage is (44.69 % and 43.25 % RH, respectively), which is slightly lower than that found using desorption data (50.10 % and 49.86 %), respectively.

4.2.4. Freundlich sorption analysis

Freundlich's model excellently describes sorption onto a surface from aqueous media and gas sorption of porous surfaces. Freundlich isotherm model is suitable for heterogeneous adsorbent surfaces multilayer adsorption. Moreover, it also accounts for the intermolecular interactions between

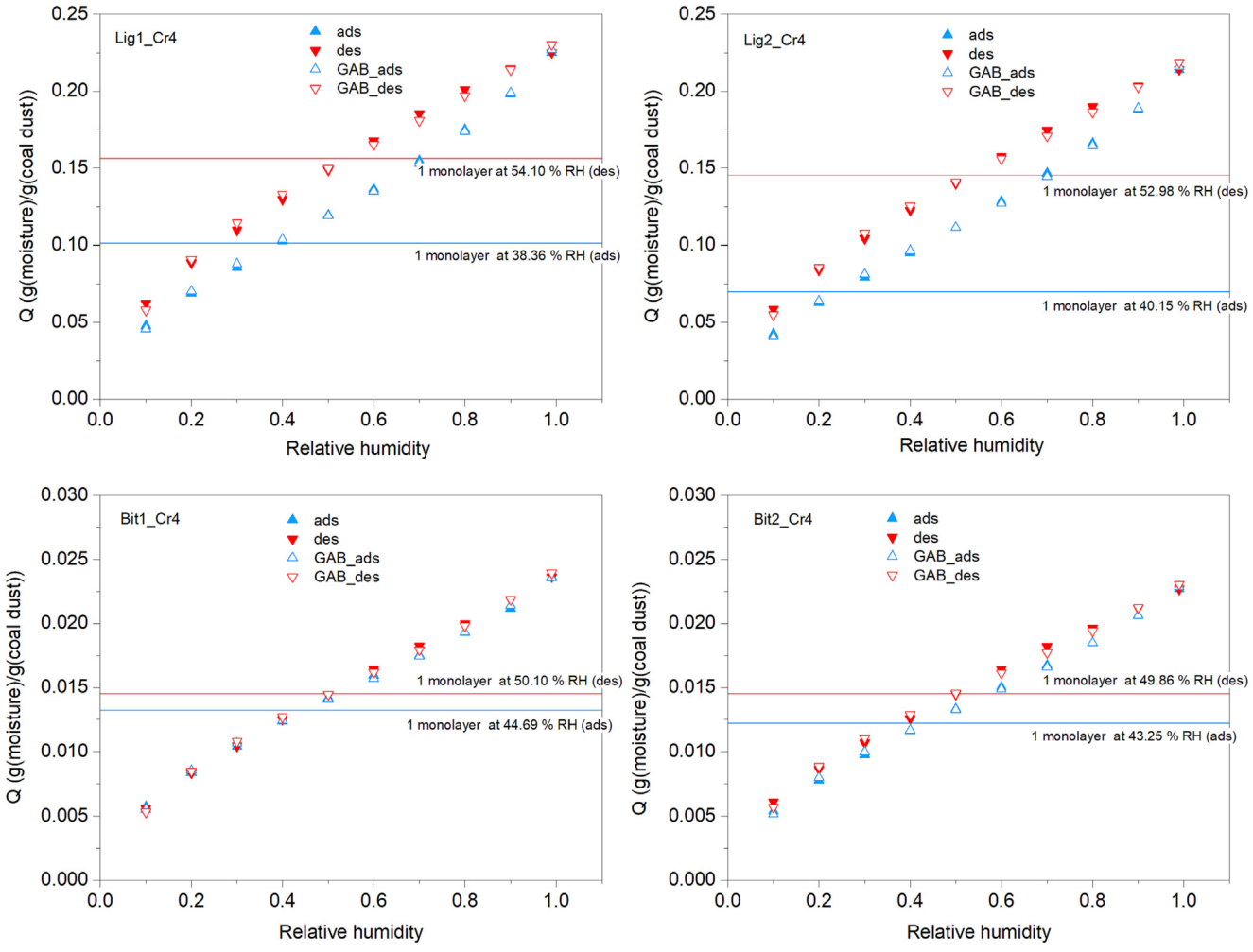

Fig. 7. Ad-/desorption isotherm obtained from the DVS and GAB fit. (ads, des represents adsorption and desorption isotherms collected from the DVS data; GAB_ads, GAB_des represents adsorption and desorption calculated using GAB method).

adsorbates (Mahmoud et al., 2021). Since coal is a heterogeneous material, the Freundlich model was used to understand its moisture interaction behavior. Eq. (6) represents the mathematical form of the Freundlich model:

$$\frac{x}{m} = k_f \left(\frac{P}{P_o}\right)^{1/n_f} \tag{6}$$

where $\frac{x}{m}$ is the concentration of the adsorbed water at equilibrium; k_f and n_f are the Freundlich empirical constants recovered from regression of the adsorption data and representing the sorption capacity and sorption strength, respectively. The linear form of the Freundlich isotherm model is given in equation Eq. (7):

$$\ln\left(\frac{x}{m}\right) = \ln k_f + \frac{1}{n_f} \ln R_h \tag{7}$$

Fig. 8 shows the experimental water adsorption data on the four coal dust samples and the corresponding values derived from the linear form of the Freundlich adsorption model. Fig. 8 demonstrates that the Freundlich model fits well with DVS data and also the goodness of fit (R_F^2) are always >98 %, as mentioned in Table 2. It is observed that, in general, a value of n_f >1, indicates a strong affinity for water vapor (Sang et al., 2019). Table 2 shows that the values of n_f are always >1, meaning a stronger affinity for water vapor for all the nano-sized coal dust samples.

Also, the k_f values representing adsorption capacity (net adsorption at RH = 99 %) calculated from the model (Table 2) are in good agreement, although slightly lower than the observed values (Table S4). There is an interesting and crucial observation that needs special mention. We found that the SSA_{GAB} for the two bituminous coal dust samples are almost ten times lower than the two Lignite coal dust samples, as mentioned in Table 1. Also, while comparing the adsorption capacity observed in the DVS experiment (Table S4) or that calculated from GAB (Table 1) or the Freundlich model (k_f) (Table 3), it was observed that the lignite coal dust samples have a much higher adsorption capacity.

Despite that, it was found that the adsorption strength is almost similar for bituminous and lignite dust. This points to the fact that the SSA of coal is not the primary determinant of water vapor sorption on coal. Rather water sorption of coal is a complex phenomenon and depends upon the surface composition of the oxygen-containing functional groups and their porosity (Liu et al., 2021). Table S1 shows that bituminous coal has lower oxygen content (4.01 % and 4.38 %) than the two-lignite coal (17.76 % and 15.32 %). This means that the oxygen-containing functional group locations are the key points where water molecules get adsorbed and form a primary layer over which secondary layers form (Do and Nicholson, 2015; Fletcher et al., 2007). So, more oxygen content in the lignite coal dust means more adsorption (hydrophilic) sites for water molecules. In contrast, less oxygen in the two bituminous coal implies fewer hydrophilic sites for water molecule adsorption. This reasoning can be more clearly understood in Fig. 9.

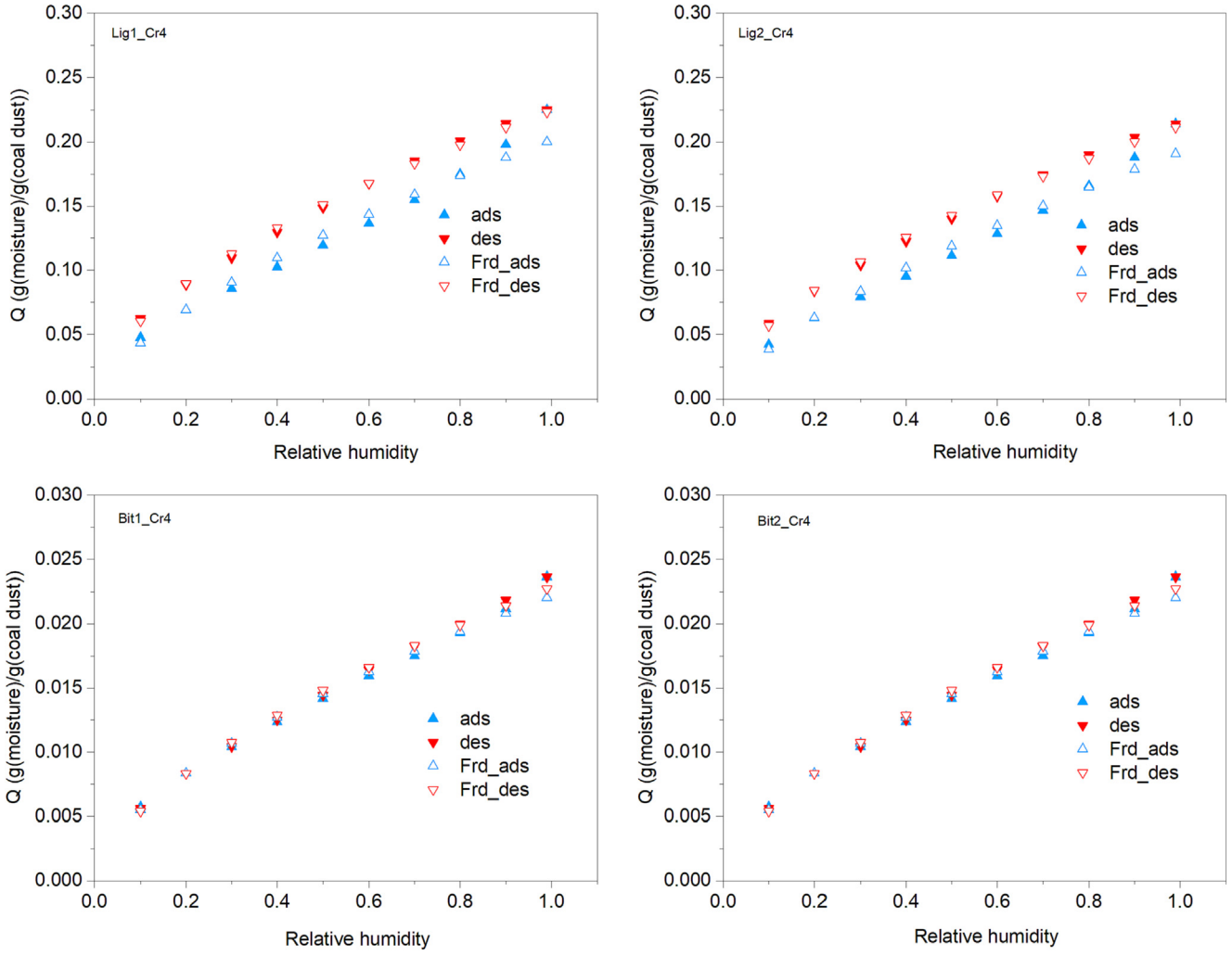

Fig. 8. Ad-/desorption isotherm obtained from the DVS and Freundlich fit. (ads, des represents adsorption and desorption isotherms collected from the DVS data; Frd_ads, Frd_des represents adsorption and desorption calculated using Freundlich method).

Table 2
Freundlich Modeling parameters of adsorption and desorption isotherms (0–0.99) for different coal dust sample.

Coal dust samples	Adsorption			Desorption		
	Model values		Goodness of fit	Model values		Goodness of fit
	k_F	n_F	R_F^2	k_F	n_F	R_F^2
Lig1_Cr4	0.2014	1.5051	98.17	0.2245	1.7526	99.75
Lig2_Cr4	0.1922	1.4407	98.40	0.2127	1.7404	99.79
Bit 1_Cr4	0.0222	1.6491	99.44	0.0229	1.5940	99.69
Bit 2_Cr4	0.0212	1.6130	99.20	0.0222	1.7259	99.61

Table 3
Total specific volume of the condensed phase found using Gurvich rule.

Sample name	$V_{Gurvich}$ (cm^3/g)
Lig1_Cr4	0.2261
Lig2_Cr4	0.2151
Bit1_Cr4	0.0237
Bit2_Cr4	0.0228

Fig. 9 shows that the oxygen-containing molecules are the key sites for the adsorption of water molecules on the coal dust. Furthermore, the adsorption of water molecules on coal dust surfaces is of two types. Type I binding between water molecules and Type II binding between a water molecule and coal dust surface. Primary bonds are formed on the surface depending on the characteristic of coal dust. This means that despite the adsorption capacity depending upon the number of adsorption sites, adsorption affinity will be similar unless the chemical structures on these adsorption sites differ. However, this is not as simple as described here, and it has been observed that the interaction between the adjacent water molecules could affect the monolayer and multilayer formation (Do and Nicholson, 2015). Nevertheless, almost similar n_F values meaning almost similar adsorption affinity observed in this study for both bituminous and lignite coal dust seem to justify the above explanation.

4.2.5. Gurvich volume

Gurvich rule is commonly used to derive the (total) specific pore volume of an adsorbent from the maximum sorption capacity (i.e., where $p/p^o \approx 1$). Gurvich's rule is based on the assumptions that: (a) the entire pore system is filled at relative pressures close to saturation pressure; (b) the adsorbate has the same physicochemical properties as its liquid-like state at operational temperature. In other words, the isotherm approaches a limiting plateau because the entire pore space is occupied by condensed adsorbate (Seemann et al., 2017). The mathematical expression for the Gurvich rule is as follows:

$$V_{Gurvich} = \frac{Q_{max}}{1000} V_m \tag{8}$$

where, $V_{Gurvich}\left(\frac{cm^3}{g}\right)$ is the total specific volume of the condensed phase, $Q_{max}\ \left(\frac{mmol}{g}\right)$ is the maximum sorption capacity, $V_m\ \left(\frac{cm^3}{mol}\right)$ is the liquid molar volume of water at the operational temperature. In this work $V_{Gurvich}$ was derived at $p/p^o = 0.99$. Table 3 shows the $V_{Gurvich}$ for different coal dust calculated using DVS isotherm data. It can be seen that the $V_{Gurvich}$ is at least 10 times higher for the two-lignite coal dust samples when compared to the two bituminous coal samples. It implies that the lignite coal dust has a much higher potential for water adsorption partically because of more oxygen containing surface sites in it. On these oxygen containing sites on the surface the water molecules mainly attaches. This can be

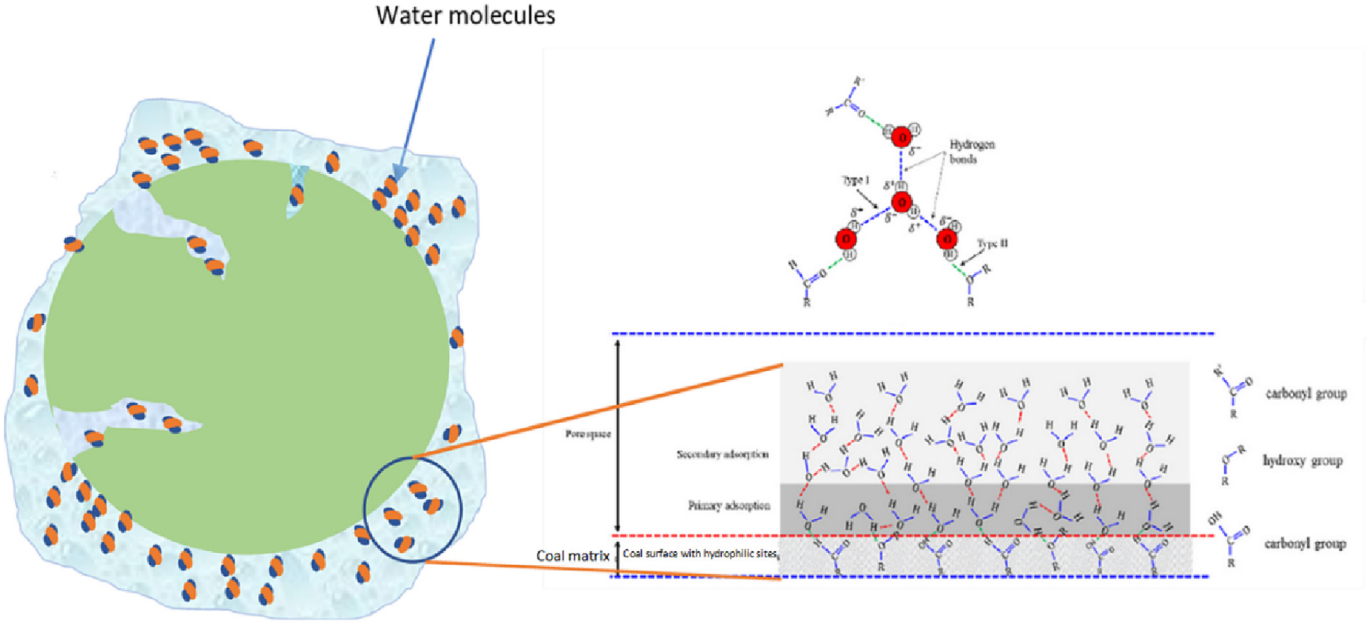

Fig. 9. Schematic representation of the water adsorption on coal dust. There are two different type of binding: Type I binding between water molecules and Type II binding between a water molecule and coal dust surface. Primary bonds are formed on the surface depending on the characteristic of coal dust.

partially explained by Fig. 9. However, there is a caveat because the water molecule is polar and hence adsorption sites of water molecules are selective, mainly oxygen-containing functional groups. So, the $V_{Gurvich}$ calculated using water vapor connects to the quantity of those specific water adsorption sites rather than providing the actual surface area for which non-polar molecules are better options.

4.2.6. Model selection and applicability for water vapor and coal dust interactions

Coal dust has a complex internal structure that changes from coal to coal. The mineral matters and pore size distribution in coals also influence water vapor sorption. This section will compare the three adsorption models (BET, GAB and Freundlich) used in the present study to calculate the water sorption isotherms for the nano-sized coal dust samples. Fig. 10 demonstrates the ad-/desorption values observed in the DVS compared to those estimated from the three models. It clearly shows that the BET model does not adequately describe the water ad-/desorption behavior of nano-sized coal dust considered in the present study. The deviation from the observed values started beyond the relative humidity of 40 % for all four samples. At high relative humidities (>70 %), BET values become excessively out of line with the observed values. Thus, the BET model does not represent the experimental results for any coal dust studied at high RH values.

Fig. 10 indicates that the GAB and Freundlich adsorption modeled results agreed well with the experimental data for all three coal dust samples studied, particularly at the higher RH values where the BET model fails. The differences may be because of the excessively simple approach of the BET model and the underlying assumptions on which it is based. Coal dust has a microporous structure (Qi et al., 2017; Zhang et al., 2020). It has been observed that the BET method is not straightforwardly applicable to materials with micro-porosity (Thommes and Cychosz, 2014). It is extremely difficult to distinctly identify the monolayer-multilayer adsorption and micropore filling processes (Thommes and Cychosz, 2014). BET model follows a layer-by-layer water uptake approach for any material. Thus, it misses other crucial aspects, such as capillary filling of wedge-shaped meso- and macropores.

In comparison, the GAB model is a modified version of the layer-by-layer approach of the BET model. As discussed, it introduces an additional term, *k*, characterizing the state of the sorbed molecules beyond the first layer. This explains the upswing systematically found in the BET plots after the initial (pseudo) linear range. Timmermann systematically checked whether BET or GAB values are physically realistic (Timmermann, 2003). His detailed study showed that there are mathematical and physical reasons for the differences in the multilayer values predicted from the two models and that the GAB values are more realistic. This means that the GAB constants must be taken as the representative multilayer sorption parameters unless it can be experimentally shown that the value of k is almost unity. In our case, the value of k is never unity as calculated from the GAB model analysis (Table S6). Also, coal dust is a heterogeneous material. This adsorption heterogeneity is not considered in the BET model, whereas Freundlich models account for the heterogeneity of the adsorption sites and intermolecular interactions. Overall, the above discussion and Fig. 10

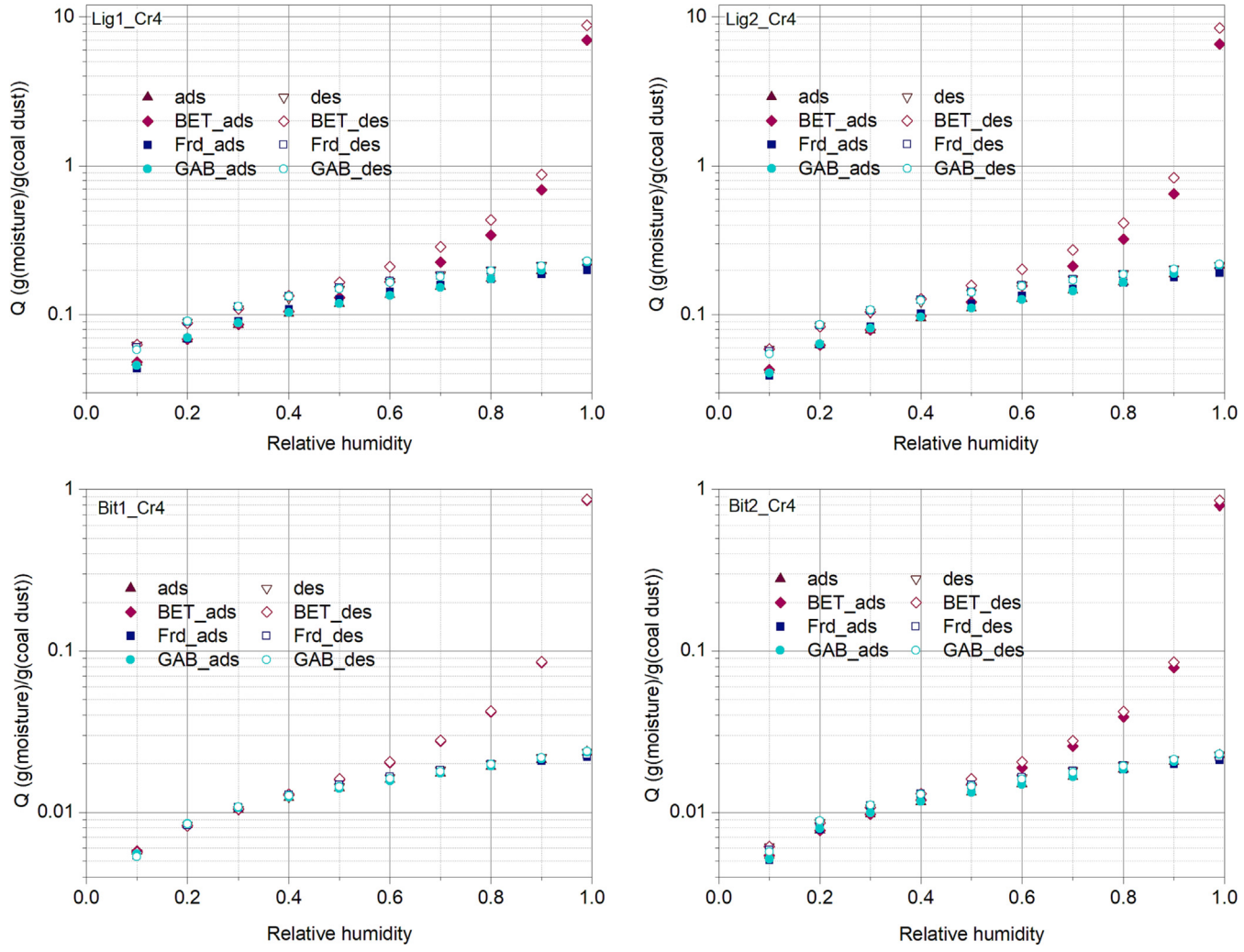

Fig. 10. Comparison of DVS sorption data with calculated BET, GAB and Freundlich model.

suggest that there is no appreciable difference between the calculations of the GAB and Freundlich model. The GAB model could provide physically realistic values for the multilayer sorption parameters. In contrast, the Freundlich model can provide adsorption potential and adsorption capacity at both low and high relative humidities. Therefore, it is recommended that both the GAB and Freundlich model can be used to define the water vapor uptake of nano-sized bituminous and lignite coal dust.

5. Discussion and implications of dust transport in underground mine environments

One of the most critical implications of coal dust and moisture is its flow behavior in the moisture environment. Several processes determine the flow and the interaction of the particles suspended in a fluid involving momentum, mass and energy. All these processes simultaneously depend on how fluid views and particle or equivalently how the particle views the fluid that surrounds it. It is understandable that the way how fluid and environment looks into each other will be significantly different under a less and high moisture conditions (Seinfeld and Pandis, 2016). Moisture dynamics of mine environment will affect particle and environment and simultaneously their interaction with each other.

Similarly, the presence and the dynamics of moisture in the flow environment could impact the flow of coal dust. If the water is absorbed, it can lead to a physicochemical change in the coal dust particles. These physicochemical changes will be dependent on the physical (size, porosity etc.) and chemical (hydrophilicity, oxygen containing functional groups etc.) characteristics of the coal dust. Moreover, water adsorption onto the surface of the coal dust particles will depend on the hydrophilic properties of the powder. Adsorbed surface water can change the interparticle forces by changing the distance between the particles and finally, the van der Waals forces, and by formation of liquid bridges. This will lead to the agglomeration of coal dust particles leading to the change of flow behavior of coal dust particles in a humid environment (Sandler et al., 2010). Also, while transporting in a humid environment moisture can also simply be integrated into the coal particle which will affect the overall specific gravity of the particle.

Some of the key components of particle flow modeling are particulate dust properties, drag forces exerted on the fluid by the particles, the specific gravity of the particles, and the motion of the coal dust particle through the air due to an imposed external force resulting from the bombardment of the particle by the molecules of the air and moisture (Seinfeld and Pandis, 2016). This section briefly discusses how the water vapor uptake of coal dust will impact the fate of dust transport behaviors in the underground mine environment.

It has been observed that the size of the particles in the atmosphere could depend upon the atmosphere's moisture and the particles' hygroscopicity (Jung et al., 2021; Zhang et al., 2010). Table 4 shows the surface coverage (θ) of the Lig1_Cr4, Lig2_Cr4, Bit1_Cr4, and Bit2_Cr4 coal dust samples calculated from the adsorption and desorption isotherms. Surface coverage was calculated using Eq. (9).

$$\theta = \frac{Q_{m(GAB)} . N_A . A_w}{SSA_{GAB}} \tag{9}$$

where θ is the surface coverage, $Q_{m(GAB)}$ is the mmol/g of moisture of the adsorbed water calculated using the GAB model for each relative humidity step, N_A, is the Avogadro's constant $\left(6.023 \times 10^{23}\right)$, A_w is the surface area of each molecule of water $\left(1.015 \times 10^{-15}\ cm^2\right)$.

The surface coverage calculated from the adsorption isotherm is always higher than those calculated from the desorption isotherm for every RH step. This is the reason that the SSA_{GAB} calculated from the adsorption is lower than those calculated from the desorption values, as shown in Table 1.

We see that surface coverage keeps on increasing as the RH increases. It suggests that whenever there are humidity changes in the environment, the size of the individual aerosols will be affected, as shown in Fig. 11. The relation between the particle size of the coal dust and moisture is complex because it involves both physisorption and chemisorption with the complex coal molecule. Overall, moisture adsorption on coal dust can be understood as a two-step process, i.e., primary and secondary adsorption. Primary adsorption is mainly dependent upon the characteristics of coal. Hydrogen bonds formed on coal dust surfaces with hydrophilic sites are termed primary adsorption. Further attachment of water molecules on the primary adsorption sites is termed secondary adsorption (Fig. 9). The primary adsorption depends mainly on the hydrophilicity of the coal dust. Hence, coal dust with a more hydrophilic nature will adsorb more moisture than coal dust with a less hydrophilic nature. In this study, we discussed that lignite is more hydrophilic in nature. Hence, it will have more potential sites for physical- and chemisorption, whereas bituminous is comparatively hydrophobic in nature.

Table 4
Surface coverage calculated from the GAB model (0–0.99) for different coal dust sample.

Relative humidity	Lig1_Cr4		Lig2_Cr4		Bit1_Cr4		Bit2_Cr4	
	ads	des	ads	des	ads	des	ads	des
0.1	0.47	0.40	0.44	0.40	0.433	0.39	0.44	0.42
0.2	0.68	0.57	0.65	0.57	0.63	0.57	0.63	0.59
0.3	0.85	0.70	0.82	0.72	0.79	0.72	0.79	0.73
0.4	1.013	0.83	0.986	0.84	0.93	0.86	0.95	0.86
0.5	1.18	0.95	1.15	0.96	1.07	0.997	1.09	0.997
0.6	1.35	1.07	1.33	1.08	1.21	1.13	1.23	1.13
0.7	1.53	1.19	1.52	1.20	1.32	1.26	1.37	1.25
0.8	1.73	1.29	1.72	1.30	1.46	1.38	1.51	1.35
0.9	1.96	1.37	1.95	1.40	1.60	1.51	1.69	1.46
0.99	2.22	1.44	2.217	1.47	1.77	1.63	1.86	1.56

Although it seems like a subtle change of dust mass, it can significantly modify the mean free path and collisions while these particles are traveling in the dynamic humid environment. Davis showed that the effective mean free path of "A" particles λ_{AB}, in a binary mixture of "A" and "B" can be given by (Davis, 1982):

$$\lambda_{AB} = \frac{1}{\sqrt{2}\pi\sigma_A^2 N_A + \pi(1+z)^{1/2} N_B \sigma_{AB}^2} \tag{10}$$

where, λ_{AB} is the mean free path of the particles, σ_A and σ_{AB} are the collision diameters for binary collisions between molecules of A and between molecules of A and B, respectively, N_A Is the number of the particle 'A' per unit volume, N_B is the number of particles 'B' per unit volume, z is the ratio of molecular masses of A and B. In Eq. (10), we observe that the mean free path of the particles is inversely proportional to the collision diameters. Adding more layers of water molecules on the nano-sized coal dust particles with the increase in the RH An extremely large amount of these particles per unit volume will have a more pronounced effect on their flow than the equivalent large-size coal dust particles. Large coal particles will have larger collision diameters; hence, the overall mean free path will decrease and vice-versa. Consequently, there are increased odds of collisions at higher humidity among the coal dust particles, further impacting the agglomeration and deposition rate during their transport. Based on the above explanation, it is clear that the coal dust particles could undergo multiple changes in their structure because of adsorption mechanisms along with the development of water film and swelling, as explained earlier. In the present study, it was observed that lignite adsorbs comparatively higher moisture than bituminous. This means that the dynamic moisture in the environment will have more impact on the physical characteristics of lignite coal dust, including particle size. Also, the surface adsorption of moisture will affect the flow behavior of particles by increasing the drag force. It will also cause an increase in the agglomeration state of coal dust particles in the environment. This will lead to an increase in the deposition rate of the coal dust particles in the environment.

The changes in the size of the particles because of RH will also affect the drag forces exerted on them. Drag forces are always present if the particles

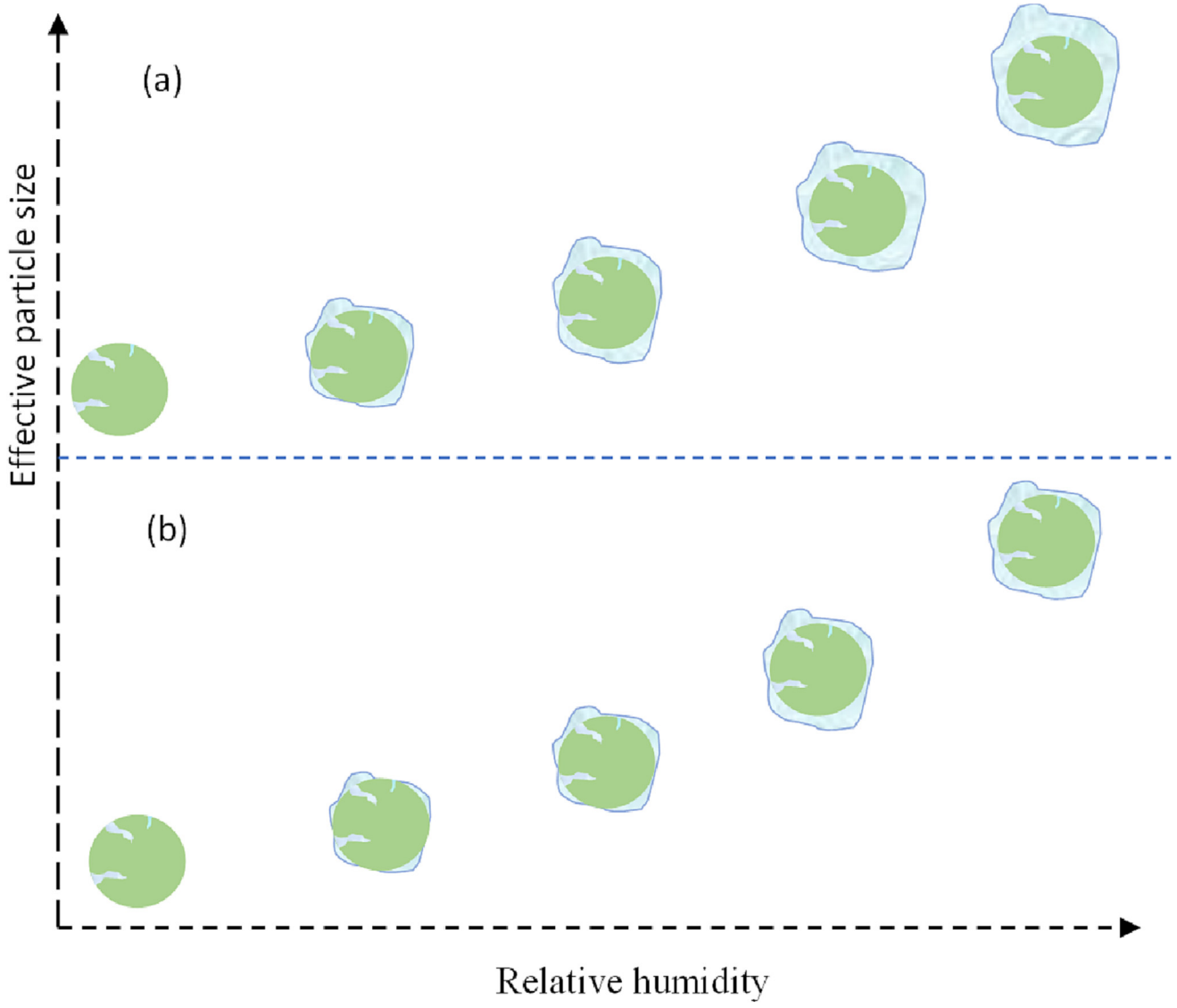

Fig. 11. Schematic representation of the impact of the RH on the particle sizes of (a) lignite and (b) bituminous coal dust, respectively.

are not moving in the vacuum. One needs to solve particle motion equations for the fluid to find actual drag forces on the coal dust particles, which involves solving the complex Navier-Stokes equation. However, to provide an understanding and if we assume that the coal dust particles are uncharged and the only driving force is the gravitational force, then the 1D momentum equation in the vertical direction for a single particle can be written as (Mallios et al., 2020):

$$m_p \frac{du_p}{dt} = m_p g - F_{drag} - F_{buoyancy} \tag{11}$$

where, m_p is the particle mass, u_p is the relative velocity of the particle in the fluid, g is the acceleration due to gravity, F_{drag} and $F_{buoyancy}$ is the magnitude of the drag force and buoyant forces acting on the particle, respectively. Now the F_{drag} is proportional to the radius of the particle (Seinfeld and Pandis, 2016) and the $F_{buoyancy}$ is proportional to the volume of the particle (Mallios et al., 2020). It can be easily understood that any changes in the particle diameters and volume because of changes in the RH will impact drag and buoyant forces on the particles. Consequently, it will affect the fate of coal dust transport in the air, as shown in Fig. 12.

Another key component of Eq. (11) is the mass of the coal dust particle is "m_p". We can set $m_p = \rho_p V_p$, where ρ_p is the specific gravity V_p is the volume of the particle, respectively. It was already discussed how the volume of the coal dust particles would change due to moisture dynamics. Another way the humidity in the air could impact the coal dust particles is by impacting their specific gravity. It is well known that particle size and

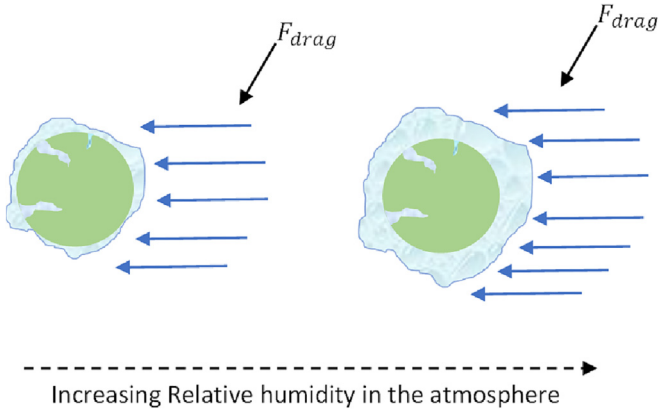

Fig. 12. Effect of relative humidity on the drag forces on individual coal dust particles.

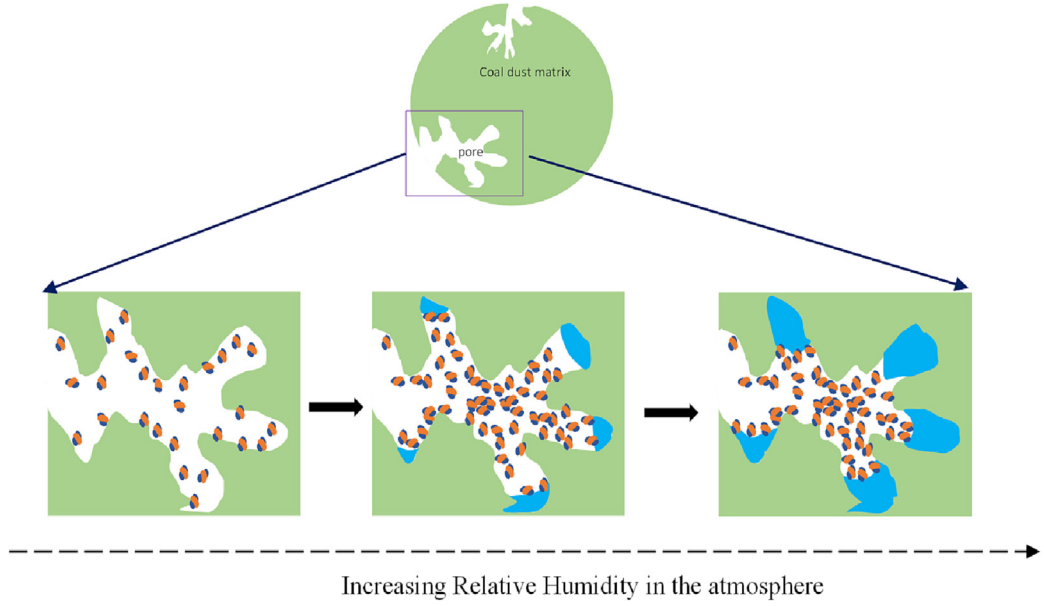

Fig. 13. Impact of the change in the relative humidity of the atmosphere on the porosity of the individual coal dust particles.

porosity are the key factors influencing the hygroscopic behavior of mineral particles (Kumar et al., 2002). Further, the porosity and particle size could evolve depending on the RH of the environment in which the coal dust particles are transported within and through. The water molecules can penetrate inside the pores of the coal dust particles, capillary condensation will occur, and higher humidity will certainly fill up some of the pores. As a result of filling the pores accessible to the water molecules, the specific gravity of the coal dust particles will change as a factor of the RH of the environment, as shown in Fig. 13. The filling up of pores and attachment of more and more water molecules with the increase in the humidity of the flow environment will increase the density of the individual coal dust particles in the atmosphere. Also, the changes will be observed more for the lignite coal dust particles than the bituminous coal dust particles.

So far, we have discussed how the properties of coal dust particles in the moisture would change because of the humidity dynamics in the environment. Another key point is that the flow of the coal dust particles is also impacted by the fluid molecules (air). The fluid molecules keep colliding with the dust particles, and such collisions are more prominent when the size of the aerosol particles is comparable to the fluid molecules. So, the air and the aerosol particle motion need to be accounted for simultaneously when the air is in motion. It can be observed that as the humidity of the flow environment increases, there is the addition of water molecules in it. This means that the coal dust particles will have an increased number of collisions per unit volume of the flow environment, as shown in Fig. 14. Because of an increased number of collisions between the coal dust particles and other molecules around, there will be comparative changes in the flow of coal dust particles. So, on one side, the properties of the particles, such as the particle size, specific gravity, and drag forces on the particles. Conversely, the flow environment is getting modified because of the humidity changes. These changes can potentially change the flow and deposition dynamics of the coal dust particles in the humified environment.

Thus, it will be crucial to account for the humidity while modeling the dust transport behavior in the underground mine environment to suppress the dust. The variations in the properties of the particles and the environment because of relative humidity can intrinsically impact the flow and deposition behaviors of coal dust particles. Further dust transport research needs to be conducted by considering the environmental variables and dust-water interactions.

6. Summary and conclusions

In this study, we conducted nano-sized coal dust and water vapor interaction experiments to understand the dynamics of water vapor uptake behaviors. We also employed different vapor sorption models to define water uptake behaviors. Four nano-sized coal dust samples were prepared

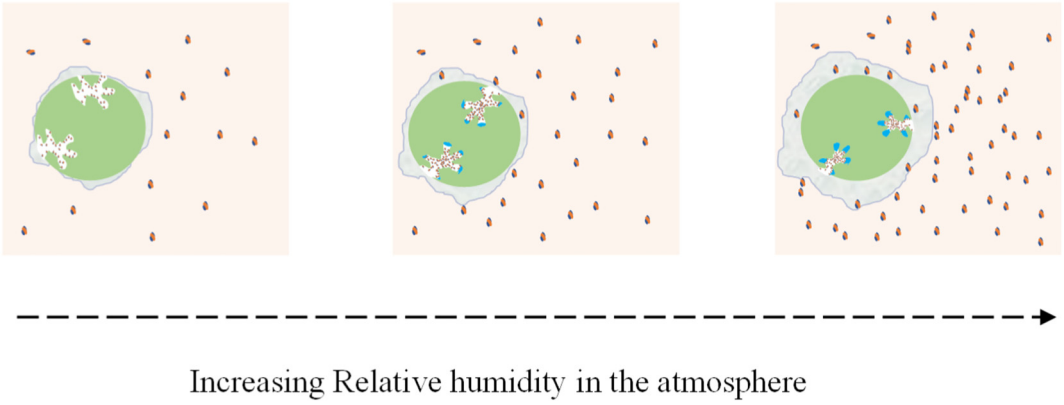

Fig. 14. Increasing quantity of water molecules in the atmosphere around the coal dust particles due to increasing RH.

from different bituminous and lignite coals. Using dynamic water vapor uptake measurements, the following conclusions can be made:

(1) It was found that there is a large difference in the water adsorption tendencies for the prepared coal dust. The two lignite coal dust samples were found to be adsorbing moisture around 10 times the bituminous coal dust samples.
(2) Three well-known adsorption models were employed to describe the water uptake behavior: BET, GAB and the Freundlich isotherms model. GAB and Freundlich models are superior to BET models for defining water uptakes.
(3) The oxygen functional group (indicated by oxygen content) plays a major role in water uptake and holding capacity on nano-size coal dust.
(4) There will be significant changes in the physical characteristics of nano-size coal dust because of interaction with atmospheric moisture, particularly because of swelling, adsorption, moisture retention, and particle size changes. This will affect the transport and deposition behavior of coal dust in the mine atmosphere.

The water uptakes can determine the fate of dust transport in an underground dynamic humidity environment. The properties of the coal dust particles could be passively altered by water uptake such as particle size, drag forces and the particles' specific gravity. This study implies that future dust transport modeling should not ignore the moisture-dust interactions toward the dust suppression application.

CRediT authorship contribution statement

SL and SA designed the research; SA and AL performed the experiments; SA analyzed and interpreted the data; SA drafted the manuscript. SL and SB gave feedback and contributed to the writing of the manuscript. All authors read and approved the final manuscript.

Data availability

Data will be made available on request.

Declaration of competing interest

The authors declare that they have no competing interests.

Acknowledgment

This work was financially supported by The National Institute of Occupational Safety and Health (NIOSH) under contract No. 75D30119C05128.

Appendix A. Supplementary data

Supplementary data to this article can be found online at https://doi.org/10.1016/j.scitotenv.2023.164095.

References

Anderson, R.B., 1946. Modifications of the Brunauer, Emmett and Teller equation 1. J. Am. Chem. Soc. 68, 686–691.
Arthur, E., Tuller, M., Moldrup, P., Greve, M.H., Knadel, M., de Jonge, L.W., 2018. Applicability of the Guggenheim–Anderson–Boer water vapour sorption model for estimation of soil specific surface area. Eur. J. Soil Sci. 69, 245–255. https://doi.org/10.1111/EJSS.12524.
Bedjanian, Y., Romanias, M.N., el Zein, A., 2013. Uptake of HO2 radicals on Arizona test dust. Atmos. Chem. Phys. 13, 6461–6471. https://doi.org/10.5194/ACP-13-6461-2013.
Brunauer, S., Emmett, P.H., Teller, E., 1938. Adsorption of gases in multimolecular layers. J. Am. Chem. Soc. 60, 309–319. https://doi.org/10.1021/JA01269A023.
Buchner, F., Forster-Tonigold, K., Bozorgchenani, M., Gross, A., Behm, R.J., 2016. Interaction of a self-assembled ionic liquid layer with graphite(0001): a combined experimental and theoretical study. J. Phys. Chem. Lett. 7, 226–233. https://doi.org/10.1021/ACS.JPCLETT.5B02449/SUPPL_FILE/JZ5B02449_SI_001.PDF.
Castro-Marcano, F., Lobodin, V.v., Rodgers, R.P., McKenna, A.M., Marshall, A.G., Mathews, J.P., 2012. A molecular model for Illinois no. 6 Argonne premium coal: moving toward capturing the continuum structure. Fuel 95, 35–49. https://doi.org/10.1016/J.FUEL.2011.12.026.
Chen, L., Peng, C., Gu, W., Fu, H., Jian, X., Zhang, H., Zhang, G., Zhu, J., Wang, X., Tang, M., 2020. On mineral dust aerosol hygroscopicity. Atmos. Chem. Phys. 20, 13611–13626. https://doi.org/10.5194/ACP-20-13611-2020.
Cheng, W., Xue, J., Xie, J., Zhou, G., Nie, W., 2017. A model of lignite macromolecular structures and its effect on the wettability of coal: a case study. Energy Fuels 31, 13834–13841. https://doi.org/10.1021/ACS.ENERGYFUELS.7B01267.
Crowley, J.N., Ammann, M., Cox, R.A., Hynes, R.G., Jenkin, M.E., Mellouki, A., Rossi, M.J., Troe, J., Wallington, T.J., 2010. Evaluated kinetic and photochemical data for atmospheric chemistry: volume v -heterogeneous reactions on solid substrates. Atmos. Chem. Phys. 10, 9059–9223. https://doi.org/10.5194/ACP-10-9059-2010.
Davis, E.J., 1982. Transport phenomena with single aerosol particles. Aerosol Sci. Technol. 2, 121–144. https://doi.org/10.1080/02786828308958618.
DEBOER, J.H., 1953. The Dynamical Character of Adsorption. LWW.
Do, D.D., Nicholson, D., 2015. Characterization of oxygen functional groups on carbon surfaces with water and methanol adsorption. Carbon N Y 81, 447–457. https://doi.org/10.1016/J.CARBON.2014.09.077.
Du, X., Wang, N., 2021. Investigation into adsorption equilibrium and thermodynamics for water vapor on montmorillonite clay. AIChE J., e17550 https://doi.org/10.1002/AIC.17550.
Fan, L., Liu, S., 2021. Respirable nano-particulate generations and their pathogenesis in mining workplaces: a review. Int. J. Coal Sci. Technol. 1–20. https://doi.org/10.1007/s40789-021-00412-w.
Fletcher, A.J., Uygur, Y., Mark Thomas, K., 2007. Role of surface functional groups in the adsorption kinetics of water vapor on microporous activated carbons. J. Phys. Chem. C 111, 8349–8359. https://doi.org/10.1021/JP070815V/SUPPL_FILE/JP070815VSI20070402_093025.PDF.
Grau, R.H., Krog, R.B., 2008. Using Mine Planning and Other Techniques to Improve Ventilation in Large-Opening Mines.
Guggenheim, E.A., 1966. Applications of Statistical Mechanics. Clarendon P.
Hatch, C.D., Wiese, J.S., Crane, C.C., Harris, K.J., Kloss, H.G., Baltrusaitis, J., 2012. Water adsorption on clay minerals as a function of relative humidity: application of BET and Freundlich adsorption models. Langmuir 28, 1790–1803. https://doi.org/10.1021/LA2042873.
He, K., Huo, H., Zhang, Q., 2003. Urban air pollution in China: current status, characteristics, and progress. 27, 397–431. https://doi.org/10.1146/annurev.energy.27.122001.083421.
He, Y., Gu, Z., Lu, W., Zhang, L., Okuda, T., Fujioka, K., Luo, H., Yu, C.W., 2019. Atmospheric humidity and particle charging state on agglomeration of aerosol particles. Atmos. Environ. 197, 141–149. https://doi.org/10.1016/J.ATMOSENV.2018.10.035.
Hudson, P.K., Young, M.A., Kleiber, P.D., Grassian, V.H., 2008. Coupled infrared extinction spectra and size distribution measurements for several non-clay components of mineral dust aerosol (quartz, calcite, and dolomite). Atmos. Environ. 42, 5991–5999. https://doi.org/10.1016/j.atmosenv.2008.03.046.
Ibrahim, S., Romanias, M.N., Alleman, L.Y., Zeineddine, M.N., Angeli, G.K., Trikalitis, P.N., Thevenet, F., 2018. Water interaction with mineral dust aerosol: particle size and hygroscopic properties of dust. ACS Earth Space Chem. 2, 376–386. https://doi.org/10.1021/ACSEARTHSPACECHEM.7B00152.
Ikhu-Omoregbe, D.I.O., 2007. Comparison of the sorption isotherm characteristics of two cassava products. 9, 167–177. https://doi.org/10.1080/10942910600592026.
JB, C., AG, W., Y, L., F, X., H, L., KA, M., TJ, C., Y, W., JB, H., 2018. Urban-rural county and state differences in chronic obstructive pulmonary disease - United States, 2015. MMWR Morb. Mortal. Wkly Rep. 67, 205–211. https://doi.org/10.15585/MMWR.MM6707A1.
Jiang, B., Sun, Q., Ni, G., 2020. Study on the wettability of a composite solution based on surface structures of coal. ACS Omega 5 (43), 28341–28350. https://doi.org/10.1021/ACSOMEGA.0C04345.
Johansen, R.T., Dunning, H.N., 1957. Water-vapor adsorption on clays. Clays Clay Miner. 6, 249–258. https://doi.org/10.1346/CCMN.1957.0060119 1986 6:1.
Joshi, N., Romanias, M.N., Riffault, V., Thevenet, F., 2017. Investigating water adsorption onto natural mineral dust particles: linking DRIFTS experiments and BET theory. Aeolian Res. 27, 35–45. https://doi.org/10.1016/J.AEOLIA.2017.06.001.
Jung, C.H., Yoon, Y.J., Um, J., Lee, S.S., Han, K.M., Shin, H.J., Lee, J.Y., Kim, Y.P., 2021. Approximated expression of the hygroscopic growth factor for polydispersed aerosols. J. Aerosol Sci. 151, 105670. https://doi.org/10.1016/J.JAEROSCI.2020.105670.
Kossovich, E.L., Borodich, F.M., Epshtein, S.A., Galanov, B.A., 2020. Indentation of bituminous coals: fracture, crushing and dust formation. Mech. Mater. 150, 103570. https://doi.org/10.1016/J.MECHMAT.2020.103570.
Kovtun, A., Jones, D., Dell'Elce, S., Treossi, E., Liscio, A., Palermo, V., 2019. Accurate chemical analysis of oxygenated graphene-based materials using X-ray photoelectron spectroscopy. Carbon N Y 143, 268–275. https://doi.org/10.1016/J.CARBON.2018.11.012.
Kumar, P., Jasra, R.v., Bhat, T.S.G., 2002. Evolution of porosity and surface acidity in montmorillonite clay on acid activation. Ind. Eng. Chem. Res. 34, 1440–1448. https://doi.org/10.1021/IE00043A053.
Li, Q., Lin, B., Zhao, S., Dai, H., 2013. Surface physical properties and its effects on the wetting behaviors of respirable coal mine dust. Powder Technol. 233, 137–145. https://doi.org/10.1016/J.POWTEC.2012.08.023.
Liu, T., Liu, S., 2020. The impacts of coal dust on miners' health: a review. Environ. Res. https://doi.org/10.1016/j.envres.2020.109849.
Liu, A., Liu, S., Liu, P., Wang, K., 2021. Water sorption on coal: effects of oxygen-containing function groups and pore structure. Int. J. Coal Sci. Technol. 1–20. https://doi.org/10.1007/s40789-021-00424-6.
Löndahl, J., Massling, A., Pagels, J., Swietlicki, E., Vaclavik, E., Loft, S., 2010. Size-resolved respiratory-tract deposition of fine and ultrafine hydrophobic and hygroscopic aerosol

particles during rest and exercise. 19, 109–116. https://doi.org/10.1080/08958370601051677.
Lu, N., Asce, F., Khorshidi, M., Asce, S.M., 2015. Mechanisms for soil-water retention and hysteresis at high suction range. J. Geotech. Geoenviron. 141, 04015032. https://doi.org/10.1061/(ASCE)GT.1943-5606.0001325.
Mahmoud, R.K., Taha, M., Zaher, A., Amin, R.M., 2021. Understanding the physicochemical properties of Zn–Fe LDH nanostructure as sorbent material for removing of anionic and cationic dyes mixture. Sci. Rep. 11, 1–19. https://doi.org/10.1038/s41598-021-00437-w 2021 11:1.
Mallios, S.A., Drakaki, E., Amiridis, V., 2020. Effects of dust particle sphericity and orientation on their gravitational settling in the earth's atmosphere. J. Aerosol Sci. 150, 105634. https://doi.org/10.1016/J.JAEROSCI.2020.105634.
Michel, A.E., Usher, C.R., Grassian, V.H., 2003. Reactive uptake of ozone on mineral oxides and mineral dusts. Atmos. Environ. 37, 3201–3211. https://doi.org/10.1016/S1352-2310(03)00319-4.
National Academies of Sciences, E. and M, 2018. Monitoring and sampling approaches to assess underground coal mine dust exposures. Monitoring and Sampling Approaches to Assess Underground Coal Mine Dust Exposures. https://doi.org/10.17226/25111.
Oching, W.E., Ghomshei, M.M., 2019. Effective Mine Ventilation Management Without Compromising Mine Health & Safety and Productivity.
Ocieczek, A., Zieba, M., 2020. Comparison of the sorption properties of fruit powder shampoos using the BET, GAB, and Peleg models. ACS Omega 5, 14354–14359. https://doi.org/10.1021/ACSOMEGA.0C00851.
Pritchard, C., 2010. Methods to Improve Efficiency of Mine Ventilation Systems.
Qi, L., Tang, X., Wang, Z., Peng, X., 2017. Pore characterization of different types of coal from coal and gas outburst disaster sites using low temperature nitrogen adsorption approach. Int. J. Min. Sci. Technol. 27, 371–377. https://doi.org/10.1016/J.IJMST.2017.01.005.
Rouquerol, J., Llewellyn, P., Rouquerol, F., 2007. Is the bet equation applicable to microporous adsorbents? Stud. Surf. Sci. Catal. 160, 49–56. https://doi.org/10.1016/S0167-2991(07)80008-5.
Rouquerol, J., Rouquerol, F., Llewellyn, P., Maurin, G., Sing, K.S.W., 2013. Adsorption by powders and porous solids: principles, methodology and applications. Second Edition, Second. edIn: Second Edition (Ed.), Adsorption by Powders and Porous Solids: Principles, Methodology and Applications. Elsevier Inc. https://doi.org/10.1016/C2010-0-66232-8.
RP, S., PJ, B., 1999. Mechanisms and mediators in coal dust induced toxicity: a review. Ann. Occup. Hyg. 43, 7–33. https://doi.org/10.1016/S0003-4878(98)00069-6.
Rubasingheghe, G., Grassian, V.H., 2013. Role(s) of adsorbed water in the surface chemistry of environmental interfaces. Chem. Commun. 49, 3071–3094. https://doi.org/10.1039/c3cc38872g.
Sandler, N., Reiche, K., Heinämäki, J., Yliruusi, J., 2010. Effect of moisture on powder flow properties of theophylline. Pharmaceutics 2, 275. https://doi.org/10.3390/PHARMACEUTICS2030275.
Sang, G., Liu, S., Elsworth, D., 2019. Water vapor sorption properties of Illinois shales under dynamic water vapor conditions: experimentation and modeling. Water Resour. Res. 55, 7212–7228. https://doi.org/10.1029/2019WR024992.
Seemann, T., Bertier, P., Krooss, B.M., Stanjek, H., 2017. Water vapour sorption on mudrocks. Geol. Soc. Lond., Spec. Publ. 454, 201–233. https://doi.org/10.1144/SP454.8.
Seinfeld, J.H., Pandis, S.N., 2016. Atmospheric Chemistry and Physics: From Air Pollution to Climate Change. 3rd ed. John Wiley & Sons, Inc.
Seisel, S., Pashkova, A., Lian, Y., Zellner, R., 2005. Water uptake on mineral dust and soot: a fundamental view of the hydrophilicity of atmospheric particles? Faraday Discuss. 130, 437–451. https://doi.org/10.1039/B417449F.
Sing, K.S.W., 1985. Reporting physisorption data for gas/solid systems with special reference to the determination of surface area and porosity (recommendations 1984). Pure Appl. Chem. 57, 603–619. https://doi.org/10.1351/PAC198557040603.
Tang, M., Cziczo, D.J., Grassian, V.H., 2016. Interactions of water with mineral dust aerosol: water adsorption, hygroscopicity, cloud condensation, and ice nucleation. Chem. Rev. https://doi.org/10.1021/acs.chemrev.5b00529.
Thommes, M., Cychosz, K.A., 2014. Physical adsorption characterization of nanoporous materials: progress and challenges. Adsorption 20, 233–250. https://doi.org/10.1007/S10450-014-9606-Z/FIGURES/11.
Timmermann, E.O., 2003. Multilayer sorption parameters: BET or GAB values? Colloids Surf. A Physicochem. Eng. Asp. 220, 235–260. https://doi.org/10.1016/S0927-7757(03)00059-1.
Triantafyllou, A.G., Zoras, S., Evagelopoulos, V., 2006. Particulate matter over a seven year period in urban and rural areas within, proximal and far from mining and power station operations in Greece. Environ. Monit. Assess. 122, 41–60. https://doi.org/10.1007/S10661-005-9162-9 2006 122:1.
Tu, K.W., Knutson, E.O., 1984. Total deposition of ultrafine hydrophobic and hygroscopic aerosols in the human respiratory system. undefined 3, 453–465. https://doi.org/10.1080/02786828408959032.
Usher, Courtney R., Michel, Amy E., Grassian, Vicki H., 2003. Reactions on mineral dust. Chem. Rev. 103, 4883–4939. https://doi.org/10.1021/CR020657Y.
Vaida, V., 2011. Perspective: water cluster mediated atmospheric chemistry. J. Chem. Phys. 135, 020901. https://doi.org/10.1063/1.3608919.
Varghese, S.K., Gangamma, S., 2009. Particle deposition in human respiratory system: deposition of concentrated hygroscopic aerosols. Inhal. Toxicol. 21, 619–630. https://doi.org/10.1080/08958370802380792.
Wang, H., Zhang, L., Wang, D., He, X., 2017. Experimental investigation on the wettability of respirable coal dust based on infrared spectroscopy and contact angle analysis. Adv. Powder Technol. 28, 3130–3139. https://doi.org/10.1016/J.APT.2017.09.018.
Wei, J., Xu, X., Jiang, W., 2020. Influences of ventilation parameters on flow field and dust migration in an underground coal mine heading. Sci. Rep. 10, 1–17. https://doi.org/10.1038/s41598-020-65373-7 2020 10:1.
Xu, C., Wang, D., Wang, H., Xin, H., Ma, L., Zhu, X., Zhang, Y., Wang, Q., 2017. Effects of chemical properties of coal dust on its wettability. Powder Technol. 318, 33–39. https://doi.org/10.1016/J.POWTEC.2017.05.028.
Yalcin, S.E., Legg, B.A., Yeşilbaş, M., Malvankar, N.S., Boily, J.F., 2020. Direct observation of anisotropic growth of water films on minerals driven by defects and surface tension. Sci. Adv. 6, eaaz9708.
Yang, J., Wu, X., Gao, J., Li, G., 2010. Surface characteristics and wetting mechanism of respirable coal dust. Min. Sci. Technol. (China) 20, 365–371. https://doi.org/10.1016/S1674-5264(09)60209-X.
Yao, Q., Xu, C., Zhang, Y., Zhou, G., Zhang, S., Wang, D., 2017. Micromechanism of coal dust wettability and its effect on the selection and development of dust suppressants. Process Saf. Environ. Prot. 111, 726–732. https://doi.org/10.1016/J.PSEP.2017.08.037.
Yu, X., Zhao, Y., Feng, Y., Hu, X., Liu, J., Wang, X., Wu, M., Dong, H., Liang, Y., Wang, W., Tian, F., 2022. Synthesis and performance characterization of a road coal dust suppressant with excellent consolidation, adhesion, and weather resistance. Colloids Surf. A Physicochem. Eng. Asp. 639, 128334. https://doi.org/10.1016/J.COLSURFA.2022.128334.
Zhang, R., Khalizov, A., Wang, L., Hu, M., Xu, W., 2010. Nucleation and Growth of Nanoparticles in the Atmosphere. https://doi.org/10.1021/cr2001756.
Zhang, Z., Qin, Y., Yi, T., You, Z., Yang, Z., 2020. Pore structure characteristics of coal and their geological controlling factors in eastern Yunnan and Western Guizhou, China. ACS Omega 5, 19565–19578. https://doi.org/10.1021/ACSOMEGA.0C02041.
Zhang, R., Liu, S., Zheng, S., 2021. Characterization of nano-to-micron sized respirable coal dust: particle surface alteration and the health impact. J. Hazard. Mater. 413, 125447. https://doi.org/10.1016/j.jhazmat.2021.125447.